



# HHS Public Access

Author manuscript

*Nat Rev Chem.* Author manuscript; available in PMC 2023 May 12.

Published in final edited form as:

*Nat Rev Chem.* 2023 May ; 7(5): 355–373. doi:10.1038/s41570-023-00476-z.

## Detection and analysis of chiral molecules as disease biomarkers

Yaoran Liu<sup>1</sup>, Zilong Wu<sup>2,3,✉</sup>, Daniel W. Armstrong<sup>4,✉</sup>, Herman Wolosker<sup>5,✉</sup>, Yuebing Zheng<sup>1,2,3,6,✉</sup>

<sup>1</sup>Department of Electrical and Computer Engineering, The University of Texas at Austin, Austin, TX, USA.

<sup>2</sup>Walker Department of Mechanical Engineering, The University of Texas at Austin, Austin, TX, USA.

<sup>3</sup>Texas Materials Institute, The University of Texas at Austin, Austin, TX, USA.

<sup>4</sup>Department of Chemistry & Biochemistry, University of Texas at Arlington, Arlington, TX, USA.

<sup>5</sup>Department of Biochemistry, Rappaport Faculty of Medicine, Technion-Israel Institute of Technology, Haifa, Israel.

<sup>6</sup>Department of Biomedical Engineering, The University of Texas at Austin, Austin, TX, USA.

### Abstract

The chirality of small metabolic molecules is important in controlling physiological processes and indicating the health status of humans. Abnormal enantiomeric ratios of chiral molecules in biofluids and tissues occur in many diseases, including cancers and kidney and brain diseases. Thus, chiral small molecules are promising biomarkers for disease diagnosis, prognosis, adverse drug-effect monitoring, pharmacodynamic studies and personalized medicine. However, it remains difficult to achieve cost-effective and reliable analysis of small chiral molecules in clinical procedures, in part owing to their large variety and low concentration. In this Review, we describe current and emerging techniques that detect and quantify small-molecule enantiomers and their biological importance.

### Graphical Abstract

---

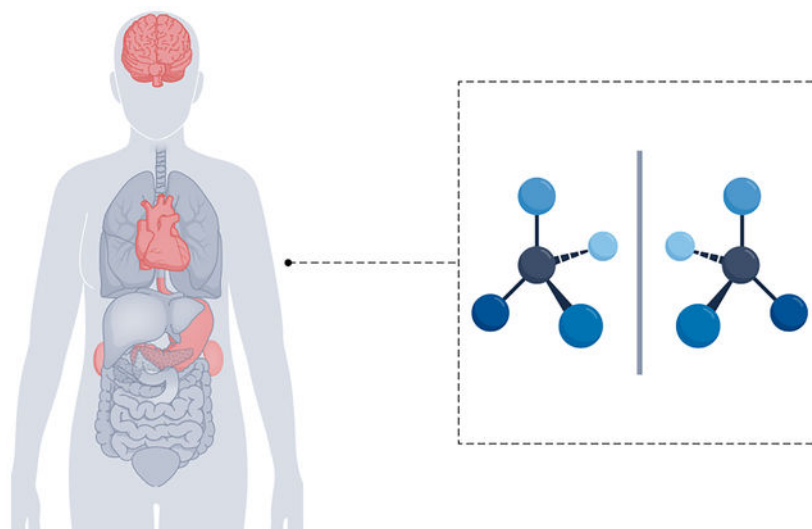
✉ zlwu@utexas.edu; sec4dwa@uta.edu; hwoloske@technion.ac.il; zheng@austin.utexas.edu.

#### Author contributions

All authors collected data, wrote and edited the manuscript. Y.L. drafted the manuscript. D.W.A and H.W. provided substantial content. Y. L., Z. W. and Y. Z. conceived the content, and edited and finalized the manuscript.

#### Competing interests

The authors declare no competing interests.



## Introduction

The identification and detection of distinct biomarkers is important for the diagnosis of disease, evaluating disease progression and even the development of therapeutics<sup>1–3</sup>. Small molecules (<1,000 Da) — for example, sugars, fatty acids and amino acids — are gaining prominence as novel biomarkers<sup>4</sup>, largely owing to the ‘omics’ revolution in the past decade<sup>5</sup>. In contrast to other biomarkers, such as proteins and genetic materials, small molecules can reflect not only downstream results of the genome but also upstream inputs from drugs. This allows scientists to monitor the onset and progress of diseases, as well as responses to drugs<sup>6</sup>.

An advantage of small-molecule biomarkers is that many of them are chiral<sup>7</sup>. Such molecules are referred to as enantiomers, which can be said to exist in ‘right-handed’ and ‘left-handed’ forms. Common chiral small molecules in humans (and other species) include carbohydrates (for example, glucose), organic acids (for example, lactate and 2-hydroxyglutarate (2-HG)) and amino acids (for example, serine, aspartate and alanine)<sup>8</sup>. Normally, chiral molecules with specific types of ‘handedness’ will dominate over the other types in biological systems<sup>9</sup>. For example, chiral amino acids exist mainly as L-enantiomers, whereas the D-enantiomers of carbohydrates are dominant in all living things<sup>10</sup>. Such basic chemical components are fundamental for stereoselective protein formation. The chirality of these small molecules also affects biochemical processes, such as molecular binding, molecular synthesis and signalling in cell communication<sup>11</sup>. Interestingly, the chirality of small molecules depends on the physiological status of animals, including humans. Internal or external influential factors (Fig. 1), such as toxins, mutations, racemization, enzyme deficiencies, infection and radiation, can induce enantioselective changes, leading to abnormal chirality of molecules in biofluids or tissues<sup>12–14</sup>.

Because of the strong correlation between molecular chirality and pathological processes, abnormal concentrations of chiral small molecules are increasingly being identified as biomarkers for disease monitoring and treatment<sup>15,16</sup>. For example, many types of cancer

cells have a greater enantiomeric excess of D-2-HG than healthy cells. These small molecules can be used for disease prognosis and can be used to inform the most effective treatment approach<sup>17</sup>. Similarly, the determination of the D-enantiomers of glutamine and isoleucine may help identify patients with early gastric cancer for surgery or specific chemotherapies<sup>16,17</sup>. Diabetic complications and sepsis are linked to enantiomers of lactate, the measurement of which has the potential to identify patients who are candidates for intensive therapies<sup>18</sup>. The other main disease area in which chiral small molecules are implicated is brain disease. For example, D-serine (D-Ser) accounts for one third of the total serine in the brain<sup>19,20</sup> and works as a physiological ligand of a key neurotransmitter receptor, *N*-methyl-D-aspartate receptor (NMDAR)<sup>21–24</sup>. This D-amino acid is synthesized by serine racemase<sup>25</sup> and has release mechanisms<sup>26,27</sup> and catabolic pathways<sup>28,29</sup>. D-Ser is associated with the pathophysiology of several diseases, including traumatic brain injury<sup>30,31</sup>, stroke damage<sup>32</sup>, neuropsychiatric disorders<sup>33,34</sup>, epilepsy<sup>35,36</sup> and amyotrophic lateral sclerosis<sup>37,38</sup>, and is a potential biomarker for renal disease<sup>39</sup>. These are just a few examples that demonstrate the importance of measuring the enantiomeric composition of specific molecules in the diagnosis and prognosis of diseases, monitoring of drug effects and prediction of patient responses to treatments<sup>40</sup>.

This Review focuses on how chiral biomarkers are identified and analysed using the different molecular measurement techniques available. First, we describe the identification of chiral biomarkers and their correlations with diseases, followed by the difficulties in measuring low enantiomeric concentrations in clinical settings. We then discuss the working principles, strengths and limitations of the different analytical methods. We conclude by discussing the challenges and future perspectives of existing methods in achieving cost-effective and accurate detection and identification of enantiomers for biomedical research and clinical applications.

## Chiral molecules in diseases

There are two major strategies for discovering and identifying chiral biomarkers. One is to hypothesize the existing potential chiral biomarkers based on chirality-dependent physiological pathways and then to validate the hypothesis through targeted biomarker detection<sup>41</sup>. The other strategy is to identify metabolites (a subset of which are chiral small-molecule biomarkers) in human bodies in an untargeted way<sup>42</sup>. Chiral biomarkers can then be identified by establishing correlations between metabolite profiles and disease status<sup>43,44</sup>. In this section, we discuss established correlations between chiral biomarkers and diseases for three categories of disease (brain diseases, kidney disease and diabetes, and cancer), and how these biomarkers were identified.

### Brain physiology and pathology

NMDARs are major excitatory receptors in the brain and are activated by the binding of glutamate to GluN2 and a co-agonist to the GluN1 subunit<sup>45</sup>. The binding events between endogenous neurotransmitters and NMDARs in synapses are pivotal for neurotransmission<sup>23,45,46</sup>. Overstimulation or hypofunction of NMDARs by endogenous modulators can lead to synaptic dysfunction and cognitive impairments<sup>47</sup>. Recent studies

have shown that certain amino acids and chiral organic acids can enantioselectively bind to NMDARs. In this section, we review the most important of these: D-Ser, D-aspartate (D-Asp), D-alanine (D-Ala), D-lactate and L-2-HG and D-2-HG.

**D-Serine.**—D-Ser, but not L-Ser, binds to the co-agonist site of NMDARs, resulting in activation of the channel<sup>21,22,48</sup>. Targeted deletion of serine racemase — the biosynthetic enzyme for D-Ser — leads to NMDAR hypofunction and behavioural abnormalities<sup>49–51</sup>, indicating that maintaining a proper concentration of D-Ser in the brain is critical to modulate neurotransmission. However, overstimulation of the NMDARs through excessive D-Ser and glutamate leads to massive calcium influx into the cells and promotes neurotoxicity<sup>52,53</sup>. D-Ser-mediated cell death through NMDAR activation has been associated with several brain diseases, including stroke, epilepsy, chronic pain, amyotrophic lateral sclerosis and Alzheimer disease<sup>54,55</sup>. By contrast, NMDAR hypofunction caused by low D-Ser concentrations can lead to cognitive impairments, reminiscent of diseases such as schizophrenia<sup>33,50,56</sup> or normal ageing<sup>57–59</sup>. Low D-Ser concentrations have also been reported in disorders of serine biosynthesis, such as 3-phosphoglycerate dehydrogenase deficiency and phosphoserine phosphatase deficiency<sup>60</sup>. The understanding of the role of D-Ser in such biochemical processes gave researchers the impetus to detect it in human biosamples.

D-Ser has been tested as a therapeutic agent for the treatment of schizophrenia and has been shown in murine models and human patients to improve several schizophrenia symptoms when used in combination with conventional antipsychotics<sup>61–66</sup>. For example, the administration of D-Ser to mice improves recognition tasks and working memory<sup>64</sup>. Moreover, in patients with schizophrenia, the serum concentrations of D-Ser are positively associated with cognitive gains induced by intensive cognitive training<sup>65</sup>.

D-Ser has also proved effective in the treatment of other neurological diseases and conditions. For example, a pilot randomized controlled trial found improvement in symptoms of post-traumatic stress disorder in patients who were treated with D-Ser<sup>67</sup>. Another pilot study indicated that the basal plasma concentrations of D-Ser correlate with response to the antidepressant ketamine<sup>68</sup>. In line with the decrease in brain D-Ser in ageing mice<sup>57–59</sup>, administration of D-Ser reverses the age-related decrease in cognitive flexibility and restores functional brain connectivity and neuronal morphology<sup>69</sup>.

D-Ser was proposed to be a suitable biomarker in Alzheimer disease, but the results are inconsistent. Concentrations of D-Ser in the cerebrospinal fluid (CSF) of patients were reported to increase the sensitivity and specificity of the diagnosis of Alzheimer disease<sup>70</sup>. However, much smaller or no changes were observed in another cohort of patients<sup>71</sup>. Recently, Sachi and co-workers found a correlation in a larger number of subjects between serum concentrations of D-Ser and patients with Alzheimer disease<sup>72</sup>. As an internal control, they showed that D-Asp concentrations do not change in the patients. Studies in larger cohorts and with more standardized techniques are still needed to address some of the inconsistencies in the use of D-Ser, as well as other D-amino acids, as biomarkers of Alzheimer disease.

**D-Aspartate.**—D-Asp is also found in the brain and is synthesized, at least in part, by the serine racemase<sup>73</sup>. D-Asp is mostly present in neurons and decreases rapidly in the neonatal period<sup>74</sup> owing to the expression of its catabolic enzyme D-Asp oxidase<sup>75</sup>. D-Asp also binds to the glutamate-binding site of NMDARs and, when in excess, may mediate NMDAR neurotoxicity<sup>76</sup>. Transgenic mice engineered to overexpress D-Asp oxidase during the prenatal period exhibit lower brain D-Asp and changes in brain morphology<sup>77</sup>, indicating that D-Asp has a role in normal brain development. Similar to D-Ser, people with schizophrenia have lower concentrations of D-Asp<sup>78,79</sup>, which might contribute to the NMDAR hypofunction in disease development<sup>80</sup>. In Parkinson disease, D-Asp concentrations decrease in the substantia nigra of patients<sup>81</sup>, which may reflect the loss of dopaminergic neurons in this region. Although these findings are encouraging, the use of D-Asp as a biomarker requires further research in larger patient cohorts.

**D-Alanine and other D-amino acids.**—D-Ala is a co-agonist of the glycine and D-Ser site of NMDARs<sup>82</sup>. However, physiological concentrations of D-Ala in the brain are at least one order of magnitude lower than those of D-Ser<sup>82</sup>, making it unlikely that this D-amino acid interacts physiologically with NMDARs. D-Ala has been tested as a therapeutic agent for schizophrenia but requires much higher dosages than D-Ser to achieve the same therapeutic effect<sup>83</sup>. Higher concentrations of D-Ala were detected in the white matter of brains among patients with Alzheimer disease<sup>84</sup>. However, in a rat model of Alzheimer disease, plasma D-Ala concentrations were lower than in controls. In this study, concentrations of D-Ser, D-Asp, D-leucine (D-Leu) and D-proline (D-Pro) were also lower than in controls, whereas D-phenylalanine (D-Phe) concentrations increased<sup>85</sup>. Although these observations suggest that D-amino acids may be biomarkers for Alzheimer disease, these changes are not consistent across disease models and need to be confirmed in further studies in animals and humans. The research on D-amino acid biomarkers will likely involve investigating D-cysteine (D-Cys), recently identified as a major product of serine racemase enzyme activity towards L-Cys. This endogenous D-amino acid is very high in neonatal brains and is a negative regulator of cell proliferation; its potential as a biomarker is yet to be investigated<sup>86</sup>. Despite the progress made in recent years regarding the physiological and pathological roles of D-amino acids in the nervous system, much remains to be learned about their suitability as biomarkers, in part because of the difficulties in detecting small amounts of enantiomers in various body fluids.

**L-2-Hydroxyglutarate and D-2-hydroxyglutarate.**—A strong correlation between chiral organic acids and inherited neurometabolic diseases was found in the neonatal period<sup>87</sup>. In particular, accumulation of L-2-HG and D-2-HG in body fluids can cause L-2-hydroxyglutaric aciduria and D-2-hydroxyglutaric aciduria, respectively, which are accompanied by many neurological symptoms, such as psychomotor retardation, hypotonia, ataxia and seizures<sup>17,88</sup>. In early studies, despite unclear physiological pathways, untargeted metabolic profiling in human tissues led to the discovery of correlations between L-2-HG or D-2-HG and brain diseases<sup>17</sup>. Recently, in vitro studies revealed that increased D-2-HG enhances the glutamate uptake in synaptosomes and, therefore, potentially affects the excitatory neurotransmission in the central nervous system<sup>89</sup>. Studies in transfected cells indicate that D-2-HG exerts its harmful effect by activating NMDARs and causing

dysregulation of intracellular calcium and mitochondrial dysfunction<sup>90</sup>. For L-2-HG, the pathophysiology can be similar to that of D-2-HG<sup>17</sup>. However, characteristic patterns of brain magnetic resonance imaging abnormalities and neurologic symptoms suggest that L-2-hydroxyglutaric aciduria affects different brain regions than D-2-HG. Despite intensive research on the aetiology, the pathophysiology is still under investigation<sup>17,91</sup>.

### Kidney disease and diabetes

The kidneys regulate the chemical balance of vertebrate animals by selectively filtering and reabsorbing metabolites from blood. Estimation of the glomerular filtration rate (GFR) as an indicator of kidney function is crucial for early diagnosis and follow-up of chronic kidney disease<sup>92</sup>. However, routine laboratory techniques (for example, creatinine clearance) for estimating GFR are inaccurate at high GFR values and depend on muscular mass<sup>92</sup>. Normally, L-amino acids are reabsorbed much more efficiently than D-amino acids at the proximal tubules<sup>93</sup>. D-Ser accumulates in high concentrations in urine because L-Ser displaces D-Ser during amino acid reabsorption<sup>94</sup>.

Increases in plasma D-Ser are found in renal failure caused by IgA nephritis<sup>95</sup>, diabetic nephropathy<sup>95</sup>, hypertensive nephropathy<sup>96</sup> and systemic lupus erythematosus<sup>97</sup>. For example, in one case of rapidly progressive glomerulonephritis due to systemic lupus erythematosus, the concentration of D-Ser in the patient's plasma was extremely high and comprised 19% of whole blood serine in the acute phase<sup>97</sup>. The concentration of D-Ser in the plasma better correlates with the actual GFR, which is decreased in these diseases, and is independent of common clinical factors that affect routine laboratory techniques, such as muscular mass, age and sex<sup>98</sup>. Monitoring the urinary D-Ser to L-Ser ratio rather than plasma has advantages in detecting renal failure. In an acute model of kidney ischaemia, measurement of the urinary D-Ser to L-Ser ratio was more sensitive than the serum D-Ser to L-Ser ratio and all other commonly used laboratory tests to detect renal dysfunction<sup>99</sup>. Thus, for kidney ischaemia, the measurement of D-Ser could provide a useful clinical marker that outperforms the usual assays, provided that techniques for enantiomeric detection in body fluids are widely available. It is noteworthy that the concentrations of other D-amino acids, such as D-Phe, D-tyrosine (D-Tyr), D-asparagine (D-Asn) and D-Pro, also increase in the plasma in chronic kidney injury and may represent new disease biomarkers<sup>100</sup>.

Untargeted metabolic profiling has revealed an excess of D-amino acids in patients with diabetes mellitus. In particular, the ratios between D and L-enantiomer concentrations of four amino acids (that is, alanine, valine, isoleucine and leucine) in the nails of patients with diabetes were higher than those of healthy volunteers<sup>101</sup>. One study also found increased urinary D-Phe concentrations in patients with gestational diabetes<sup>102</sup>. However, further studies are needed to confirm this finding. Given that the gut microbiome is also involved in the development of obesity and obesity-related complications, such as type 2 diabetes mellitus, it is tempting to speculate that microbiome-derived D-amino acids may have a role in the diabetic pathogenesis<sup>103</sup>. Despite this potential pathophysiological pathway, further work is needed to evaluate the utility of D-amino acids as biomarkers in diabetes mellitus. In addition, higher concentrations of two D-carboxylic acids (that is, D-lactate and L/D-2-HG) were also found in the saliva, urine and plasma of patients with diabetes<sup>104</sup>.

Moreover, elevated D-lactate — a product of methylglyoxal metabolism — can contribute to acidosis and a high anion gap (a medical term that describes the gap between negatively and positively charged electrolytes in serum) in diabetic ketoacidosis<sup>105</sup>. Interestingly, L/D-2-HG not only modulates intracellular communication, as mentioned in the previous section, but also serves as a metabolic by-product to control cell growth<sup>106,107</sup>. Given the structural similarity between 2-HG and  $\alpha$ -ketoglutarate, 2-HG is a potent competitor of  $\alpha$ -ketoglutarate at the catalytic site of metabolic enzymes<sup>108</sup>. One example is its inhibition of  $\alpha$ -ketoglutarate-dependent dioxygenases, which are critical for chromatin modifications required for normal gene expression<sup>104,109</sup>.

## Cancer

Cancer cell growth is highly influenced by the intracellular and extracellular environment. Metabolic profiling revealed abnormal concentrations of certain D-amino acids and their potential use as biomarkers for different cancer types<sup>110</sup>. For example, elevated concentrations of D-amino acids, such as D-Ala and D-Pro, in gastric juice are associated with early gastric cancer<sup>111</sup>. By contrast, the concentrations of other D-amino acids, such as D-glutamic acid (D-Glu) and D-glutamine (D-Gln), decrease in the serum of patients with hepatocellular carcinoma<sup>112</sup>. Metabolic profiling of human breast cancer cells (MCF-7) and non-tumorigenic human breast epithelial cells (MCF-10) showed upregulation of some D-amino acids in MCF-7, including D-Asp and D-Ser<sup>113</sup>.

The concentrations of D-Asp and D-Ser in some cancer cells are thought to be controlled by their synthesis by serine racemase and uptake from the extracellular medium<sup>73</sup>. Serine racemase is upregulated in colorectal adenoma and adenocarcinoma, where it produces D-Ser and also promotes cancer cell growth by dehydrating serine to pyruvate<sup>114</sup>. Many other cancer types upregulate serine racemase mRNA, but the role of serine racemase and D-Ser as biomarkers or in the pathology of these tumours remains to be investigated<sup>115</sup>. Cancer cells also overexpress neutral amino acid transporters, such as ASCT2 (also known as SLC1A5), SNAT1 (also known as SLC38A1) and SNAT2 (also known as SLC38A2)<sup>116</sup>. In addition to L-Gln, which is required for cancer growth, these transporters also use D-Ser as a substrate and can transport D-Ser into cells<sup>117</sup> and, in the case of ASCT2, exchange intracellular D-Ser for extracellular amino acids<sup>118</sup>. At high intracellular concentrations, neutral D-amino acids are degraded by D-amino acid oxidase (DAAO) into hydrogen peroxide (H<sub>2</sub>O<sub>2</sub>), ammonia and the corresponding  $\alpha$ -keto acid<sup>119,120</sup>. Given the cytotoxicity of H<sub>2</sub>O<sub>2</sub>, treatment of cancer cells with D-amino acids has been proposed as a strategy to inhibit cancer growth<sup>121</sup>. However, this enzyme is mainly expressed in the kidneys, liver and cerebellum, and there is little information on its enzymatic activity in different cancer cells<sup>122</sup>. The accumulation of D-amino acids in cancer cells suggests low endogenous degradation by DAAO in cancer tissue<sup>110</sup>.

Although NMDARs are highly expressed in the central nervous system, their upregulation also occurs in tumours and cancer cells outside the brain<sup>123,124</sup>. Blockade of NMDARs decreases cell proliferation in a wide variety of cancer cells<sup>125</sup>. Consequently, binding of D-Ser or D-Asp (either produced by cancer cells or present in the extracellular medium) to non-neuronal NMDARs could influence cancer cell proliferation<sup>126</sup>. Collectively, the

concentrations of D-amino acids may increase or decrease in different cancers, and further research is needed to evaluate their effectiveness as biomarkers and in anticancer therapy<sup>113,119,124,126–128</sup>.

The growing understanding of the biochemical consequences of protein mutations has also led to the discovery of novel chiral biomarkers. In particular, mutations of isocitrate dehydrogenase 1/2 (IDH1/2), which controls cellular metabolism, are frequently observed in various cancers such as glioma, cholangiocarcinoma, acute myeloid leukaemia, lung cancer, colorectal cancer and nasopharyngeal carcinoma<sup>129</sup>. Mutations in IDH1/2 prevent the catalytic conversion of isocitrate to  $\alpha$ -ketoglutarate, resulting in D-2-HG accumulation<sup>130</sup>. Moreover, D-2-HG inhibits  $\alpha$ -ketoglutarate-related dioxygenases, including several histone demethylases, leading to changes in DNA methylation and gene expression<sup>108,130–133</sup>.

## Summary

Identification of novel chiral biomarkers is important for developing new avenues for disease diagnosis and prognosis, as well as pharmacological studies and therapeutic innovations. The correlation between chiral biomarkers and diseases discovered by untargeted metabolic profiling may also accelerate our understanding of pathological pathways in various diseases. Table 1 summarizes many of the identified disease-related chiral biomarkers and their concentrations in various tissues and fluids. As discussed in the following sections, there are no standardized instruments and protocols for chiral measurements and data analysis. Therefore, the concentrations in different studies may vary owing to differences in sample preparation and detection methods<sup>56,72,134</sup>.

## Difficulties in clinical detection

The detection of low-concentration chiral biomarkers for diseases in clinical settings is challenging<sup>135</sup>. Herein, we discuss the main factors that make it difficult to discover new chiral biomarkers and complicate the clinical application of chiral separation techniques for known chiral biomarkers.

## Variation among chiral small molecules

There are thousands of different chiral small molecules in the human body. A technique that can specifically and accurately detect as many of these as possible is desirable for multiplexed chiral analysis to improve disease diagnosis and prognosis. However, the large variation in their molecular properties (for example, charge, mass and functional groups) makes it challenging for a single technique to be universally applied to all relevant species<sup>136,137</sup>. Further, depending on the species and the detection method, analytes may be analysed in native or derivatized forms<sup>138</sup>. There are many possible derivatization agents available, each of which has advantages and disadvantages in terms of extraction and pre-concentration, chiral separation and compatible detection approach(es). Szökő et al. provide an extensive table focusing on how the molecular properties of chiral small molecules affect the requirements and utility of the available detection techniques<sup>137</sup>. For example, different derivatization approaches in mass spectrometry are required for compounds with amine groups and those with carboxylate groups. Grossman and Colburn indicate that different



chiral selectors are required for compounds with different charge, functionality and size in capillary electrophoresis (CE)<sup>139</sup>. The effective dynamic range of cutting-edge metabolomics techniques is nearly five orders of magnitude<sup>140</sup>. However, this is still insufficient for quantification of some small chiral molecules, the concentration range of which can exceed five orders of magnitude (Table 1).

### Low concentration in clinical samples

Many chiral small molecules are present at micromolar or lower concentration in human biofluids, which necessitates the use of a highly sensitive detection technique<sup>141</sup>. Moreover, the changes in chiral biomarkers between normal and disease states may be small, especially at the onset of a disease. As shown in Table 1, the average concentration of L-2-HG in the plasma of healthy subjects and patients with cancer may differ by only 0.2  $\mu\text{M}$ . Therefore, detecting changes of 0.2  $\mu\text{M}$  or even less in enantiomeric concentration is essential in such cases for early diagnosis and prognosis of diseases. This detection limit is challenging for some existing techniques (for example, polarimetry<sup>142,143</sup>, which can barely quantify concentrations below 1  $\mu\text{M}$  (ref.<sup>144</sup>), and circular dichroism (CD) spectroscopy<sup>145</sup>).

The presence of salts in high concentration and other constituents (for example, proteins, viruses, cells, L-amino acids and D-sugars) in clinical samples can interfere in the detection of low-concentration chiral small molecules<sup>146</sup>. For example, the 22 most abundant proteins account for more than 99% of the dry mass of human plasma, with chiral small molecules making up the remaining 1% of the mass<sup>147</sup>. Therefore, it is necessary to conduct pre-detection sample preparation steps (for example, separation and filtration) to remove interfering constituents. However, poor sample preparation and pre-concentration techniques can result in the loss of low-concentration metabolites or changes in their relative concentrations, resulting in low detection sensitivities and/or inaccurate determination of the targeted metabolites in biological samples<sup>148,149</sup>.

Clinical samples collected from the human body are often limited in quantity. With the exception of urine, of which up to 1 l can be collected per day, the collection of biosamples (for example, CSF, brain tissue and blood samples) is limited in volume, and can involve pain and sometimes life-threatening risks. Specifically, because of human health-risk considerations, the maximum quantity of CSF from the brain and blood from a healthy adult human body that can be collected within a 24-h period should be below 20 ml (refs.<sup>150,151</sup>). For paediatric patients and patients in critical conditions, the acquirable sample volume is much smaller. Therefore, it is important for an effective technique to use as little biosample as possible to achieve accurate enantioselective detection. Unfortunately, some of the prevailing analytical techniques (for example, polarimetry<sup>142,143</sup> and CD spectroscopy<sup>145</sup>) cannot meet the quantity requirement for paediatric patients and patients in critical conditions.

### Frequency of testing and high cost

For some diseases, diagnosis, treatment monitoring and prognosis via detection of chiral biomarkers will require long duration and frequent testing. For example, in a mouse study, routine chiral testing over 40 h led to a deeper understanding of the pathophysiology and

biochemical consequences of renal failure<sup>99</sup>. However, comparable routine chiral testing has not been conducted on human subjects, and there is no consensus on the standardized frequency and methods of such testing. Considering the frequency of conventional chronic kidney disease and cancer testing, the potential frequency of chiral testing can vary between 0.5 and 1 year, or more often, depending on the disease severity<sup>147</sup>.

To detect chiral molecules at low concentrations (for example, <1  $\mu\text{M}$ ), costly instrumentation (for example, liquid chromatography–tandem mass spectrometry) might be necessary to achieve high sensitivity (down to picomoles) and selectivity (up to 18 chiral amino acids)<sup>152</sup>. The number of samples to be analysed per individual can be large when chronic diseases such as certain cancers and diabetes are involved, given the long duration of treatments and potential for relapse. This results in high testing costs. Tremendous efforts are required to develop high-throughput techniques that can routinely and accurately detect chiral biomarkers at lower cost to reduce the financial burden on patients and healthcare systems while increasing patient access.

## Summary

Owing to these existing challenges, there is still no standardized chiral detection technique for disease applications. Usually, there are tradeoffs in several parameters (for example, sensitivity, accuracy, speed of analysis, cost). For example, certain aromatic tagging agents can render amino acids and carboxylates fluorescent or amenable to chiral analysis<sup>137</sup>. Therefore, several chiral detection techniques have been developed to satisfy specific parameters.

## Detection techniques

In this section, we examine the existing techniques for identifying and measuring chiral biomarkers. We focus on the working principles and clinical applications of the most common of these techniques and highlight their unique features. A brief description of sample preparation is also provided because this is necessary to reduce the complexity of clinical samples for analytical chirally selective techniques.

## Sample preparation

It is often necessary to include sample preparation steps prior to the detection and analysis of small chiral molecules. Human biofluids contain millions of small and large molecules. To specifically detect the often low-concentration chiral molecules of interest, it is important to purify the sample and separate specific targeted molecules from the biofluid (Fig. 2).

**Sample collection.**—Sample collection is the first step in the detection and analysis of chiral biomarkers. The reliability of the testing depends on several environmental and human factors during collection, minor variations of which can change metabolite concentrations. Consistent collection times and fasting status are vital to maintain similar conditions for all samples. It has been shown that at least 19% of the metabolites in human plasma — especially amino acids, corticosteroids and bilirubin — exhibit substantial time-of-day variation<sup>153</sup>. The time-of-day variations in urine metabolites can be even greater than those

of plasma<sup>154</sup>. Therefore, sample collection for chiral metabolites should typically be done in the morning after 8–12 h of fasting<sup>155</sup>.

Another important factor is contamination during sample collection. Sample collection should be conducted quickly to avoid airborne contamination. Furthermore, all sample collection tubes must be kept sterile and dust-free. This is because microbial contamination can rapidly alter concentrations of small-molecule metabolites by adsorption and metabolism. In addition, dust particles are well-known sources of amino acids and adsorb many small-molecule metabolites<sup>156</sup>. Sample tubes containing plasticizers and polymers have been found to be the major sources of contamination in mass spectrometry analysis<sup>157</sup>. Depending on sample type, ethylenediaminetetraacetic acid (EDTA)-containing, heparin-containing and citrate-containing tubes are most commonly used for serum to prevent coagulation of blood in a clinical setting. In particular, EDTA sample tubes were found to present a higher content of amino acids (for example, aspartate, histidine and glutamine) than citrate ones<sup>158</sup>. Unlike serum containers, which require specialized materials, urine sample containers can be simple polypropylene tubes<sup>159</sup>.

**Sample pre-processing.**—After sample collection, pre-processing steps must be performed on samples before chiral analysis, while ensuring that the original chiral metabolite concentrations are preserved. In general, this involves centrifugation, filtration and addition of pre-servatives. The aim of centrifugation or filtration is to remove the cells, bacteria and large proteins. Typically, cells and cell debris are removed from biofluid by centrifuging at low speed (~1,000–3,000 *g*) for between 15 and 30 min (refs.<sup>160,161</sup>). Some studies showed that the centrifugation speed and time affect the metabolomic profiles of plasma samples<sup>162</sup>, whereas others showed no significant differences based on these centrifugation parameters<sup>163</sup>. It should be noted that the speed and time of centrifugation should not be too high or too long to prevent the rupturing of blood cells, which can alter the concentrations of metabolites<sup>164</sup>. After the first centrifugation, the supernatant liquid is taken. To further extract small chiral metabolites (for example, amino acids), 5–15% sulfosalicylic acid and trichloroacetic acid (TCA) should be added to the supernatant to help precipitate and remove proteins<sup>165</sup>. This is followed by a second high-speed centrifugation (~10,000–15,000 *g*)<sup>160,166</sup>. This second supernatant layer contains mostly small molecules. Further purification can be conducted through cation or anion exchangers by derivatizing polar small molecules; or using solid-phase extraction with a more hydrophobic solid phase; or by liquid–liquid extraction<sup>167</sup>.

The preparation processes for serum and plasma are similar, except that an additional coagulation process is required for serum prior to centrifugation, which has been shown to affect metabolite concentrations<sup>168</sup>. Higher lactate and amino acid amounts and lower glucose concentrations have been found in serum than in plasma<sup>169</sup>. However, there is still no general selection rule for the most suitable matrix. The bottom line is to maintain consistency of sample type throughout a study. The pre-processing procedures for urine and saliva are similar to those of serum and plasma, and also require centrifugation and TCA precipitation<sup>170–172</sup>. For tissue samples and cell cultures, extra steps before centrifugation are required to collect the desired small molecules. These steps involve the breakdown of

the tissue matrices into liquid suspensions through homogenization<sup>173</sup>. For more details, additional discussion about serum and plasma can be found elsewhere<sup>174,175</sup>.

In summary, sample preparation steps are essential for measuring chiral biomarkers. Several factors in the sample preparation, including small-molecule *recovery rates*, filtration efficiency and procedural complexity, need to be balanced to achieve accurate, reproducible and cost-effective chiral detection<sup>176</sup>. The addition of an internal standard greatly improves accuracy and reproducibility. Standardization of pre-processing approaches is still under debate and can depend on the nature of the sample and the diseases of interest.

## Chromatography

**Liquid chromatography.**—Liquid chromatography is a commonly used separation technique for small molecules<sup>177</sup>. When different small molecules in a solution migrate in a chromatography column, they are separated — owing to their different affinities towards the solid phase — and have molecule-dependent retention times. The detection and quantification of specific molecules can then be achieved by coupling the chromatography to a mass spectrometry detector or a fluorescence detector. Conventional liquid chromatography–mass spectrometry can achieve separation of molecules in a mixture based on their mass to charge ratio, but cannot distinguish between enantiomers, which have identical mass. Different separation strategies can be used to achieve enantiomeric separation and detection of small chiral molecules (Fig. 3).

The oldest approach to achieve enantiomeric separation and detection is to pre-derivatize the clinical analytes of interest with an enantiomerically pure chiral derivatization reagent (CDR) before chromatography<sup>152,178</sup>. The resulting diastereomeric products from the enantiomers can be separated based on their different affinities with the achiral stationary phase in a chromatography column. For example, a chiral *o*-phthalaldehyde-*N*-acetyl-L-cysteine CDR can react with the primary amine groups of most amino acids<sup>179</sup>. With this approach, 15 pairs of enantiomers of chiral amino acids were resolved using high-performance liquid chromatography (HPLC). Liquid chromatography with CDRs has led to the discovery of fivefold and threefold increases in the concentrations of D-Ser and D-Asp, respectively, in CSF samples from patients with Alzheimer disease, compared with healthy control groups, whereas the concentrations of L-amino acids remained almost the same<sup>180</sup>. Chiral organic acids, such as 2-HG, can be separated using *O*-acetyl-di-(*o*)-2-butyl esters as the CDR in liquid chromatography. Their use for chiral detection in urine, plasma and CSF from patients with aciduria led to the observation of a 150–200-fold increase of the measured concentration of D-2-HG, which is related to aciduria<sup>181</sup>. Liquid chromatography with a CDR also has the advantage of being low cost. Disadvantages include the requirement for the CDR to be enantiomerically pure, which is rarely the case. Reagent chiral impurities result in spurious diastereomeric peaks and poor quantification<sup>182</sup>. Incomplete derivation, for kinetic reasons, can result in altered diastereomeric ratios, and diastereomers do not have to have identical detector responses<sup>183</sup>. Moreover, not all molecules of interest have appropriate functional groups to derivatize. In addition, different CDRs need to be developed for different types of analytes. Finally, unwanted side reactions might lead to strong

background noise and interfering spectra during data acquisition. For these reasons, this approach is rarely used today.

The other strategy is to use chromatography columns with a chiral stationary phase or, less commonly, to use a chiral mobile-phase additive with an achiral stationary phase<sup>152,177</sup>. Chiral mobile phases must not interfere with detection (for example, they must be non-UV absorbing and volatile if using mass spectrometry detection) and be enantiomerically pure, as is the case for CDRs<sup>183</sup>. Moreover, a considerable amount (several grams) of the chiral mobile-phase additive may be needed for separations. Nevertheless, it has been shown that liquid chromatography with a chiral mobile phase allowed the separation and subsequent detection of 18 chiral amino acids in plasma at picomolar concentrations. Such amino acid profiling enabled the observation of clear association between Alzheimer disease and plasma concentrations of D-Ser, D-Asn, D-Asp, D-Pro, D-Leu and D-Phe<sup>85</sup>.

Liquid chromatography with a chiral stationary phase is applicable to a greater variety of small molecules than liquid chromatography with a chiral mobile-phase additive, and is often used for untargeted metabolite profiling<sup>183</sup>. Moreover, without the requirement for chiral derivatization, there are fewer sample preparation steps. In one example application of liquid chromatography with a chiral stationary phase, chiral organic acids were quantified, leading to the detection of elevated concentrations of D-2-HG in urine samples from patients with D-2-hydroxyglutaric aciduria<sup>184</sup>. It has been noted that chiral columns are also usually more expensive than achiral columns with chiral derivation. However, because individual chromatography columns are typically used for hundreds or even thousands of analyses, the cost per separation between chiral and ‘derivatized achiral’ separations is negligible.

To improve the selectivity and peak capacity of chiral separation, 2D and 3D chiral liquid chromatography techniques have been developed, in which two or three sequential columns are applied<sup>126,185–188</sup>. For example, a 2D chiral liquid chromatography that combined an achiral column and a chiral column was used to detect trace amounts of chiral metabolites, including those with enantiomeric excess below 1%<sup>187</sup>. In another example, four D-amino acids (phenylalanine, tyrosine, tryptophan and leucine), with concentrations ranging from 0.01% to 1% of the corresponding L-amino acids, were found in human urine through 2D chiral liquid chromatography that combined an octadecylsilyl column (achiral) and a Crownpak CR(+) (chiral) column<sup>188</sup>. 3D-HPLC methods have shown improved selectivity for the clinical samples over 2D-HPLC. For example, a 3D-HPLC method was developed for the determination of trace concentrations of D-Asn, D-Ser, D-Ala and D-Pro in human serum<sup>186</sup>. In this case, the extra anion-exchange column was needed as the second dimension to separate the interfering compounds from the derivatized amino acid analytes.

**Gas chromatography.**—Gas chromatography operates on an analogous principle to liquid chromatography, but requires analytes to be vapourized before they are delivered to, and separated in, a gaseous mobile phase travelling through a capillary column<sup>189</sup>. Either a CDR or a chiral stationary phase is needed for gas chromatography to achieve separation and subsequent detection of enantiomers. For example, gas chromatography with *N,O*-pentafluoropropionyl isopropyl derivatives has been applied to enantioselectively separate serine and alanine, and to determine their enantiomeric excess in blood and brain

tissues from rats<sup>20</sup>. Because gas chromatography requires volatile compounds, it is often used for compounds that contain derivatized hydroxyl, amine or carboxylate groups<sup>190</sup>. Amino acids must be doubly derivatized (that is, both the carboxylate group and the amine group must be sequentially derivatized) to obtain a sufficiently volatile product<sup>191</sup>. Typically, an ester is formed from the carboxy group and a small amide is formed from the amine functional group. When using an achiral column, one of the two derivatizing agents must be chiral. In contrast with liquid chromatography, gas chromatography often requires an additional derivation step for volatilizing the analytes into the gaseous phase.

## Capillary electrophoresis

CE separates migrating molecules of different size to charge ratios in a capillary or channel across which a high voltage is applied<sup>139</sup> (Fig. 3). After separation, a mass spectrometry or fluorescence detector is applied at the end of the channel to obtain sufficiently sensitive detection of the analytes. CE requires chiral mobile-phase additives in the running buffer in the capillary or channel to achieve enantiomeric separation and detection. CE often provides high efficiency separations and relatively short migration times, but these vary widely with the chiral mobile-phase additive used, the nature of the running buffer and the separation voltage. In one example study, the separation of ten chiral and three achiral amino acids using chiral CE was obtained in ~25 min<sup>192</sup>. CE has also been used to detect chiral amino acids and chiral drug molecules in human biofluids (for example, urine and plasma) with nanomolar sensitivity<sup>193</sup>. Chiral CE coupled with laser-induced fluorescence (CE-LIF) detection also allowed the simultaneous determination of the D-Ser and L-Ser concentrations in the midbrain tissues of a Parkinson disease mouse model<sup>194</sup>. CE-LIF has been used to detect high concentrations of D-Ser and L-Glu in single glial vesicles, indicating that these vesicles share similar biochemical features to neuronal synaptic vesicles<sup>195</sup>. CE-LIF has also been used to detect D-Asp and D-Glu in individual neurons isolated from the central nervous system<sup>196</sup>. The main advantage of chiral CE is its small sample size requirements and relatively short separation times<sup>197</sup>. However, chiral CE has relatively low sensitivity compared with chromatography and difficulties in coupling chiral CE and mass spectrometry, which result from contamination of the mass spectrometry by chiral selectors, such as cyclodextrins<sup>198</sup>. For these reasons, chiral CE is usually coupled with fluorescence detectors and used for large-molecule separations (such as proteins, peptides and oligonucleotides), and is used far less commonly than liquid chromatography for small-molecule separations in clinical settings<sup>199</sup>.

## Nuclear magnetic resonance spectroscopy

Conventional nuclear magnetic resonance (NMR) spectroscopy is a powerful technique for detecting molecular fingerprints and determining molecular structures<sup>200,201</sup>. For example, NMR spectroscopy was applied to determine the absolute configurations (that is, the chirality) of 2-HG and 5-oxoproline in human urine samples, which had strong correlations with independently diagnosed D-2-hydroxyglutaric aciduria and L-5-oxoprolineuria<sup>202</sup>. However, enantiomers of small molecules have indistinguishable conventional NMR spectra. To achieve enantiomeric detection, NMR requires either CDRs or the addition of chiral shift reagents to convert enantiomers to diastereomeric derivatives or association complexes,

respectively<sup>203</sup> (Fig. 4a). Moreover, without proper sample pre-separation, the NMR spectra are noisy, which limits the number of detectable metabolites to ~10, far from the 20 detectable with sample pre-separation and sensitivity to ~50 nM (refs.<sup>202,204</sup>). Chromatographic or electrophoretic separation as an extra sample preparation step can be coupled with chiral NMR to reduce noise and improve resolution for the detection of chiral small molecules in complex biosamples. However, if such pre-separation steps are necessary, NMR is superfluous unless it also can be used to determine the absolute configuration. Hence, there are few reports involving the use of NMR to detect and identify low-concentration chiral biomarkers of clinical importance.

### Enzymatic assays

Enzymatic assays with chiral reagents can detect targeted enantiomers of specific molecules by catalysing the chemical reaction of a specific enantiomer to a by-product<sup>205</sup>. For example, the glucose oxidase enzyme catalyses the oxidation of D-glucose, but not L-glucose, to H<sub>2</sub>O<sub>2</sub> and D-gluconolactone<sup>206</sup>. Fluorescent imaging of the by-products can be applied to determine the concentrations of the specific enantiomers (Fig. 4b). Many common chiral small molecules, including amino acids and organic acids, have well-developed enzymatic assay kits for their measurements in biofluids<sup>207</sup>. For example, a DAAO-based chemiluminescent assay was used to assess the concentrations of D-Ser in brain tissues<sup>21</sup> and to monitor online its release from living neural cells<sup>208</sup>. In another study, using purified DAAO coupled to a tyramine-based fluorescent assay, the total concentration of 14 D-amino acids in CSF was profiled and was found to be 1.48 times higher in people with Alzheimer disease than in healthy controls<sup>209</sup>. In the context of diabetes, enzymatic detection of D-Lactate in human plasma and urine uncovered a twofold increase in the D-Lactate concentrations in urine samples from people with diabetes when compared with healthy controls<sup>18</sup>. Conventional transition metals can be used to enhance the catalysis reaction without chiral selectivity<sup>210</sup>. However, by engineering chiral monodentate or multidentate ligands within the coordination sphere of the metal catalyst, it can be used to enhance the reaction for the asymmetric synthesis of nonracemic chiral compounds<sup>211</sup>, and their products can also be measured by current flow using amperometric biosensors. For example, an amperometric chiral biosensor was used to detect several D-amino acids in serum<sup>212</sup> and urine<sup>213</sup> with a better response time (<50 s) than fluorescence imaging (~ 30 min).

Because of the high selectivity, low cost, minimal sample preparation requirements and short detection times (<50 s)<sup>212,213</sup>, enzyme-based chiral sensing is widely used in measuring concentrations of chiral small molecules in biofluids and tissues for early diagnosis and prognosis of diseases, such as cancers, kidney diseases and cardiovascular diseases. However, enzyme assays usually have limited sensitivity at ~1 μM, which is above the concentration of some chiral small molecules (Table 1). In addition, the specific enzymes required are not readily available for all chiral biomarkers. For example, no L-glucose oxidase is commercially available. Moreover, enzymes often display cross-selectivity for other related molecules. For example, DAAO can react with more than one type of D-amino acid. This limits specificity and accurate quantification and makes it difficult to measure enantiomeric excess using enzymatic assays in these cases.

## Chiroptical spectroscopy

**Polarimetry.**—Polarimetry can determine the overall chirality of molecules in a solution by monitoring the degree of rotation of plane-polarized light passing through the sample<sup>144</sup> (Fig. 5). However, polarimetry has low sensitivity and additional separation or fractionation steps (for example, using chromatography and centrifugation) are required to achieve the detection of targeted chiral small molecules in complex biosamples. For example, conventional liquid chromatography with an achiral column was coupled with a polarimeter for determining the enantiomeric purity in a standard solution with a sample loading of 50  $\mu\text{g}$  and claimed enantiomeric excess accuracies of  $\pm 1\%$ <sup>142</sup>. However, if a certain chiral biomarker has a much higher concentration than other biomarkers in a sample, polarimetry can also be used to approximately quantify the enantiomeric purity without the sample separation<sup>214</sup>. For example, in vivo, real-time, non-invasive monitoring of blood chirality was demonstrated by measuring the polarimetric signals from the anterior chambers of rabbits' eyes, which showed a strong linear correlation with blood glucose (which exists in the D-form in living bodies) concentrations that were measured using glucose meters<sup>143</sup>. Overall, polarimetry has the advantages of being capable of monitoring chirality changes with good speed ( $<1$  min) and having simple sample preparation steps. Moreover, it can be used to detect analytes that do not absorb UV–visible light, if they are in sufficiently high concentrations. However, because of its limited capability of detecting enantiomeric concentrations and its limited sensitivity above 1 mM, it is rarely used to measure disease-related chiral biomarkers.

**Circular dichroism spectroscopy.**—CD spectroscopy is another chiroptical technique, which can quantify the enantiomeric excess of chiral molecules by measuring the difference in molecular absorption between left and right-handed circularly polarized light<sup>215</sup> (Fig. 5). The signs and amplitudes of the spectral peaks and troughs of the CD spectra can provide information about the enantiomeric purity of chiral molecules in a sample, although standard sample compounds and curves are required. Moreover, additional separation steps are required to detect specific chiral biomarkers<sup>216</sup>. For example, CD spectroscopy coupled with HPLC has been developed to quantify the enantiomeric excess of phenylalanine in a mixture of 15 amino acids with a detection limit of  $\sim 5 \mu\text{M}$  (ref.<sup>217</sup>).

Although it can detect the enantiomeric purity of chiral metabolites at a similar enantiomeric excess to polarimetry, CD spectroscopy is mainly used to determine the secondary and tertiary structures of chiral macromolecules, such as proteins<sup>145,218–220</sup>. For example, disease-related secondary structures of amyloid- $\beta$ -associated and amyloid light chain-associated amyloidosis can be quantified in the far-UV region<sup>221</sup>. However, as with polarimetry, extra separation and concentration steps are necessary to achieve targeted amyloidosis measurements. For example, CD spectroscopy has been used to detect amyloidosis in biofluids and tissues for brain, kidney and cancer diseases<sup>145,218,219</sup>; the lowest reported detection limit for protein in these studies was  $0.1 \text{ mg ml}^{-1}$  (ref.<sup>145</sup>).

CD spectroscopy provides more molecular information than polarimetry and has greater sensitivity for analytes that contain chromophores. However, it has poorer sensitivity and specificity than chiral liquid chromatography coupled with mass spectrometry or



fluorescence detectors. Moreover, a relatively large volume of biofluid (~1 ml) is required for CD spectroscopy<sup>145</sup>.

**Raman optical activity spectroscopy.**—Raman spectroscopy typically detects vibrational modes of molecules based on the inelastic scattering of light. The high specificity of Raman spectral shifts has allowed these shifts to be used as molecular ‘fingerprints’ to detect amino acids, protein and cells in human biofluids for diagnostic applications<sup>222</sup>. Raman optical activity (ROA) arises from the difference between the Raman spectra of molecules excited by left and right-handed circularly polarized light. The ROA spectra can reveal the absolute configuration and conformational dynamics of chiral molecules with high specificity<sup>222,223</sup> (Fig. 5). ROA spectroscopy has been used to successfully detect a wide range of chiral biomolecules, including amino acids, carbohydrates, polypeptides and nucleic acids<sup>224,225</sup>. ROA spectra provide more stereochemical information than polarimetry and CD spectroscopy. However, for clinical measurements, ROA spectroscopy requires substantial analyte enrichment because its sensitivity is limited to ~0.2 mM (ref.<sup>226</sup>). The long signal acquisition time also limits ROA’s applicability in measuring chiral biomarkers for diseases.

**Vibrational circular dichroism spectroscopy.**—Vibrational circular dichroism (VCD) spectroscopy distinguishes enantiomers by their chirality-dependent optical absorption of circularly polarized light upon the excitation of their vibrational modes<sup>227</sup>. By analysing the *g* factors (that is, asymmetry in circularly polarized light absorption) across a broad frequency range, one can quantify the enantiomeric concentrations of chiral molecules with high resolution (Fig. 5). For example, the enantiomeric excess of chiral camphor and borneol was determined by VCD spectroscopy with a resolution of 1%<sup>228</sup>. By comparing the different vibrational modes in the VCD spectra with *ab initio* calculations, the absolute configuration of chiral molecules can also be determined, leading to high molecular specificity<sup>228,229</sup>. However, similar to ROA, VCD has limited sensitivity (~5 mM) and long signal acquisition times (up to several hours)<sup>230</sup>. Methods for analyte enrichment or signal enhancement are required for VCD spectroscopy to routinely detect chiral biomarkers in clinical samples.

### Surface-enhanced chiroptical sensing

Chiroptical spectroscopic techniques have unique advantages in the enantiomeric detection of chiral small molecules and can often be used without the need for chiral derivations or added chiral selectors. However, most of them, including polarimetry, CD spectroscopy, ROA spectroscopy and VCD spectroscopy, have limited sensitivity and often require large quantities of sample, which limits their applicability in detecting low concentrations of disease-related chiral biomarkers in low-volume clinical samples. To overcome these limitations, surface-enhanced chiroptical spectroscopy has been developed.

**Surface-enhanced CD spectroscopy.**—Chiral plasmonic nanostructures, which are systems containing nanostructured metallic components that allow exploitation of surface plasmon resonances, have been used to enhance the sensitivity of CD spectroscopy for detecting small chiral molecules adsorbed to appropriate nanostructures. The enhancement

is enabled by the strong chiral electrical fields that exist near optically excited plasmonic nanostructures<sup>231,232</sup>. For example, gammadion-shaped metasurfaces, twisted nanorod metasurfaces and moiré chiral metamaterials with strong intrinsic CD signals have been applied to achieve sensitive detection of chiral molecules<sup>233–236</sup>. When chiral molecules approach metasurfaces or metamaterials, the CD spectral shifts of the metasurfaces or metamaterials with opposite handedness respond differently. The spectral shifts of left-handed and right-handed metasurfaces or metamaterials are typically represented as  $\lambda_{\text{LH}}$  and  $\lambda_{\text{RH}}$ , respectively. Depending on the absolute value of the dissymmetry factor ( $\lambda = \lambda_{\text{RH}} - \lambda_{\text{LH}}$ ), the handedness and chiral purity of the chiral molecules can be determined. Because of the enhanced sensitivity, the application of chiral metasurfaces or metamaterials for chiral molecule detection can greatly reduce the sample consumption from millilitre to microlitre amounts. Moreover, with the integration of plasmon-enhanced molecular accumulation, moiré chiral metamaterials<sup>234,235</sup> have been used to detect enantiomeric purity of chiral biomarkers, including glucose and lactate, with a sensitivity of  $\sim 100$  pM<sup>237</sup>. This higher sensitivity enabled the detection of a diabetes-induced abnormal dextrorotatory shift in the chirality of urine metabolite with a good diagnostic accuracy of 84%<sup>237</sup>. Achiral plasmonic nanostructures have also been demonstrated to enhance the CD spectroscopy of chiral small molecules<sup>238</sup>. Once chiral small molecules are adsorbed on the surfaces of achiral plasmonic nanostructures, strong CD signals are induced near the plasmonic-resonance wavelengths, leading to higher sensitivity than conventional CD<sup>231,232</sup>.

Another strategy for surface-enhanced CD spectroscopy is to use the self-assembly of plasmonic nanoparticles and chiral small molecules, whereby two or more colloidal plasmonic nanoparticles spontaneously bind with chiral molecules to form chiral metamolecules<sup>239</sup>. Such self-assembled metamolecules can exhibit strong CD signals near the plasmonic-resonance wavelengths, improving the sensitivity of CD spectroscopy. For example, cysteine was bound with gold nanoparticles to form chiral metamolecules, which enabled the enantiomeric detection of cysteine with a sensitivity of 20 pM (ref.<sup>240</sup>). Dielectric nanostructures and metasurfaces have also been demonstrated for surface-enhanced CD spectroscopy with a potentially higher figure of merit and better sensitivity than their plasmonic counterparts<sup>241</sup>.

With strongly enhanced sensitivity and drastically reduced sample consumption, surface-enhanced CD spectroscopy is a promising technique for detecting abnormal chiral biomarkers for disease diagnosis<sup>242,243</sup>. Further, the small size of plasmonic and dielectric nanostructures may lead to the development of point-of-care biomedical devices<sup>244</sup>. However, similar to conventional CD spectroscopy, proper sample separation and extraction procedures are required for surface-enhanced CD spectroscopy to be used to specifically measure a targeted chiral biomarker in complex clinical samples.

**Surface-enhanced ROA spectroscopy.**—The Raman signals of molecules can also be enhanced by plasmonic nanostructures<sup>245</sup>. This enhancement strategy has been applied to increase the intrinsically weak ROA signals of chiral small molecules. For example, L-ribose and D-ribose attached to silver–silica nanotags via covalent binding led to enhanced ROA spectra with mirror symmetry for the ribose enantiomers<sup>246</sup>. The enhancements can be up to three to six orders of magnitude greater than those of conventional ROA. In addition,

the acquisition time of surface-enhanced ROA spectroscopy is ten times shorter than that of conventional ROA spectroscopy<sup>246</sup>. Therefore, this may become a powerful tool for the detection of chiral biomarkers with high specificity. However, the reliability and the ease of spectral interpretation of surface-enhanced ROA spectroscopy need to be improved before it can be widely adopted for clinical applications.

## Challenges and opportunities

Each technique for the detection and quantification of disease-related chiral biomarkers has advantages and limitations in biomedical research and for clinical applications (Table 2). Currently, chiral liquid chromatography and 2D liquid chromatography–mass spectrometry are the most widely used approaches because of their universality of application, sensitivity and reproducibility of qualitative and quantitative data. Many new approaches, especially chiroptical spectroscopy methods, could be advantageous in terms of speed, cost per analysis and sensitivity. However, they are currently not as common as chiral liquid chromatography or 2D liquid chromatography–mass spectrometry in clinical applications. In addition, every method requires some degree of sample preparation, which is often the ‘rate limiting step’ of the analysis. In this section, we discuss the challenges and opportunities for the development of reliable analytical techniques that can be widely adopted for chiral biomarker detection in disease diagnosis and monitoring.

### Sample preparation

Proper sample preparation that can extract targeted chiral biomarkers from complex biosamples with a high recovery rate is crucial for accurate chiral detection<sup>247</sup>. This often requires the use of sophisticated sample preparation procedures<sup>248</sup>. Moreover, the large compositional, chemical and physical differences among different types of biosamples, such as urine, blood, CSF and tissues, require the sample-specific procedures<sup>249</sup>. Finally, many laboratories develop their own sample preparation procedures independently. These factors contribute to the high cost, high time consumption and low reliability of chiral biomarker detection. Therefore, standardization and automation of the sample preparation procedures will facilitate the advancement the field<sup>250</sup>. Automation is dependent on progress in the fields of microfluidics, machine learning and robotics.

### Data validation and reproducibility

Many of the spectroscopic analytical techniques for detecting chiral biomarkers in clinical samples are still in the early stages of development. In all techniques, there is a lack of standardized instruments and protocols for measurements and data analysis. Further, sample complexity and variability can lead to changeable and sometimes contradicting measurement results<sup>251</sup>. These problems need be addressed to advance the detection of chiral biomarkers into clinical practices<sup>252</sup>.

### Cost-effective and rapid detection

Because the concentrations of chiral biomarkers are strongly related to the identification and progression of many diseases, it is essential to routinely detect the variation of chiral biomarkers during diagnosis, prognosis and treatment monitoring<sup>253</sup>. Devices that can

operate at the point of care will be especially beneficial to patients with chronic diseases, including some cancers and diabetes, by reducing the cost and increasing accessibility<sup>254</sup>. Rapid detection (that is, with results produced within 1 h of sample collection) is desirable for physicians to identify diseases, identify the potential for relapse and determine treatment strategies at the earliest time to improve patient outcomes<sup>255</sup>. However, the most widely adopted techniques, such as chiral chromatography coupled with a mass spectrometer, are expensive and can be time-consuming (that is, hours to days) unless multiplexed. Moreover, they are often limited to use by experienced technicians or scientists in centralized laboratories. We expect that tremendous development in the field of point-of-care devices will lead to cost-effective and rapid detection of chiral biomarkers in the future<sup>256</sup>.

### Multiplexed detection of chiral biomarkers

Multiplexed detection (that is, simultaneous characterization and quantification of multiple biomarkers) is becoming increasingly important owing to the growing demand for untargeted profiling<sup>257</sup>. Simultaneous measurement of several chiral biomarkers is also desirable in clinical practices to increase disease specificity when the detection of a single biomarker is insufficiently sensitive. It is also desired for ruling out factors that could drive changes of a specific biomarker<sup>258</sup>. Currently, most chiroptical techniques have not achieved multiplexed detection. However, chromatography and CE can be used to analyse multiple chiral small molecules in a single sample analysis<sup>259</sup>. A challenge in simultaneously quantifying various amino acids and organic acids arises from the large amount of complex data generated by different chiral molecules within the low  $m/z$  area where there is also strong background noise<sup>260</sup>. To address the challenge for multiplexed detection, novel approaches and sensor designs are needed<sup>261</sup>. Machine learning has proved promising in complex data analysis. Its implementation in chiral detection will increase the detection accuracy and accelerate the identification of multiplexing chiral biomarker detection<sup>262</sup>.

### Sensitivity improvement

Many of the techniques for the detection of small chiral molecules have limited sensitivity, which is typically at a micromolar or milli-molar concentration (Table 2). The limited sensitivity prevents their clinical application, for which it is necessary to detect much lower concentrations of targeted chiral biomarkers to distinguish between patient groups and control groups<sup>263</sup>. The development of analytical techniques with improved sensitivity even up to the single-molecule concentration will broaden the biomedical applications of small-molecule chiral biomarkers in both scientific research and clinical settings<sup>264</sup>.

### Conclusions

'Abnormal' chirality and trace concentrations of enantiomeric small molecules are emerging as potential biomarkers for various diseases. For example, strong correlations have been observed between chiral biomarkers and life-threatening and/or chronic diseases, including brain diseases, cancers, kidney disease and diabetes, as well as for osteoporosis, inflammatory bowel disease, atherosclerosis and hypertension<sup>265,266</sup>. However, the pathophysiological mechanism of many of these chiral molecules is still unclear.

Nevertheless, these studies have provided a valuable framework for the future study of new chiral biomarkers in other diseases.

Despite considerable efforts in developing techniques for detecting chiral molecules, some are still at proof-of-concept stages. Improving the sensitivity, increasing the sample throughput and lowering the cost per analysis of these techniques are necessary for both clinical and commercial viability. These improvements will enable the discovery, verification and pathological understanding of new chiral biomarkers, as well as the clinical diagnosis and prognosis of diseases, monitoring of adverse drug effects, companion diagnosis for personalized (precision) medicine and acceleration of treatment decisions.

## Acknowledgements

Y.L., Z.W. and Y.Z. acknowledge the financial support of the National Institute of General Medical Sciences of the National Institutes of Health (NIH) (R01GM146962) and National Science Foundation (NSF) (ECCS-2001650). D.W.A acknowledges the support of the R. A. Welch Foundation (Y-0026). H.W. acknowledges the financial support of Israel Science Foundation 337/19, Ministry of Health, and Allen and Jewell Prince Center for Neurodegenerative Disorders of the Brain.

## Glossary

<b>Chiral</b>	The geometric property of a molecule that precludes it from being superimposable on its mirror image
<b>Chiral selectors</b>	Chiral components in the chiral separation system that interact enantioselectively with the target chiral molecule
<b>Chiroptical</b>	The optical properties related to the interaction of chirality
<b>Enantiomeric excess</b>	The excess of one enantiomer over the other in a mixture of enantiomers
<b>Enantiomers</b>	A pair of compounds that are not superposable onto their own mirror image
<b>Metabolites</b>	Substances produced after metabolism (food, drugs or chemical digestion)
<b>Metabolomics</b>	A systematic study of chemical processes involving metabolites, the small-molecule substrates, intermediates and products of cell metabolism
<b>Metamaterials</b>	Materials engineered to have a property that is not found in the equivalent naturally occurring materials
<b>Metasurfaces</b>	2D thin film materials that can modulate the propagation of electromagnetic waves
<b>Multiplexed</b>	A way of measuring the concentration of multiple biomarkers

**Recovery rates**

The percentages of molecular concentration that can be recovered from the total concentration after physical or chemical processes

**References**

1. Etzioni R et al. The case for early detection. *Nat. Rev. Cancer* 3, 243–252 (2003). [PubMed: 12671663]
2. Hanash SM, Pitteri SJ & Faca VM Mining the plasma proteome for cancer biomarkers. *Nature* 452, 571–579 (2008). [PubMed: 18385731]
3. Blennow K, Hampel H, Weiner M & Zetterberg H Cerebrospinal fluid and plasma biomarkers in Alzheimer disease. *Nat. Rev. Neurol* 6, 131–144 (2010). [PubMed: 20157306]
4. Rinschen MM, Ivanisevic J, Giera M & Siuzdak G Identification of bioactive metabolites using activity metabolomics. *Nat. Rev. Mol. Cell Biol* 20, 353–367 (2019). [PubMed: 30814649]
5. Rochfort S Metabolomics reviewed: a new “omics” platform technology for systems biology and implications for natural products research. *J. Nat. Prod* 68, 1813–1820 (2005). [PubMed: 16378385]
6. Gomez-Casati DF, Zanol MI & Busi MV Metabolomics in plants and humans: applications in the prevention and diagnosis of diseases. *Biomed. Res. Int* 2013, 792527 (2013). [PubMed: 23986911]
7. Quack M Structure and dynamics of chiral molecules. *Angew. Chem. Int. Ed* 28, 571–586 (1989).
8. Evans PR An introduction to stereochemical restraints. *Acta Crystallogr. D* 63, 58–61 (2007). [PubMed: 17164527]
9. Blackmond DG Autocatalytic models for the origin of biological homochirality. *Chem. Rev* 120, 4831–4847 (2019). [PubMed: 31797671]
10. Plasson R, Kondepudi DK, Bersini H, Commeyras A & Asakura K Emergence of homochirality in far-from-equilibrium systems: mechanisms and role in prebiotic chemistry. *Chirality* 19, 589–600 (2007). [PubMed: 17559107]
11. Shen Q, Wang L, Zhou H, Yu L-S & Zeng S Stereoselective binding of chiral drugs to plasma proteins. *Acta Pharmacol. Sin* 34, 998–1006 (2013). [PubMed: 23852086]
12. Müller T & Kohler H-P Chirality of pollutants — effects on metabolism and fate. *Appl. Microbiol. Biotechnol* 64, 300–316 (2004). [PubMed: 14716466]
13. Armstrong DW, Zukowski J, Ercal N & Gasper M Stereochemistry of pipecolic acid found in the urine and plasma of subjects with peroxisomal deficiencies. *J. Pharm. Biomed. Anal* 11, 881–886 (1993). [PubMed: 8305590]
14. Armstrong DW, Gasper M, Lee SH, Zukowski J & Ercal N D-Amino acid levels in human physiological fluids. *Chirality* 5, 375–378 (1993). [PubMed: 8398594]
15. Utembe W Chirality, a neglected physico-chemical property of nanomaterials? A minireview on the occurrence and importance of chirality on their toxicity. *Toxicol. Lett* 311, 58–65 (2019). [PubMed: 31054352]
16. Abdulbagi M, Wang L, Siddig O, Di B & Li B D-Amino acids and d-amino acid-containing peptides: potential disease biomarkers and therapeutic targets? *Biomolecules* 11, 1716 (2021). [PubMed: 34827714]
17. Kranendijk M, Struys EA, Salomons GS, Van der Knaap MS & Jakobs C Progress in understanding 2-hydroxyglutaric acidurias. *J. Inherit. Metab. Dis* 35, 571–587 (2012). [PubMed: 22391998]
18. Talasniemi JP, Pennanen S, Savolainen H, Niskanen L & Liesivuori J Analytical investigation: assay of D-lactate in diabetic plasma and urine. *Clin. Biochem* 41, 1099–1103 (2008). [PubMed: 18638467]
19. Hashimoto A, Oka T & Nishikawa T Extracellular concentration of endogenous free D-serine in the rat brain as revealed by in vivo microdialysis. *Neuroscience* 66, 635–643 (1995). [PubMed: 7644027]
20. Hashimoto A et al. The presence of free D-serine in rat brain. *FEBS Lett* 296, 33–36 (1992). [PubMed: 1730289]

21. Mothet J-P et al. D-Serine is an endogenous ligand for the glycine site of the N-methyl-D-aspartate receptor. *Proc. Natl Acad. Sci. USA* 97, 4926–4931 (2000). [PubMed: 10781100]
22. Le Bail M et al. Identity of the NMDA receptor coagonist is synapse specific and developmentally regulated in the hippocampus. *Proc. Natl Acad. Sci. USA* 112, E204–E213 (2015). [PubMed: 25550512]
23. Mothet JP, Le Bail M & Billard JM Time and space profiling of NMDA receptor co-agonist functions. *J. Neurochem* 135, 210–225 (2015). [PubMed: 26088787]
24. Dallérac G et al. Dopaminergic neuromodulation of prefrontal cortex activity requires the NMDA receptor coagonist D-serine. *Proc. Natl Acad. Sci. USA* 118, e2023750118 (2021). [PubMed: 34083436]
25. Wolosker H, Blackshaw S & Snyder SH Serine racemase: a glial enzyme synthesizing D-serine to regulate glutamate-N-methyl-D-aspartate neurotransmission. *Proc. Natl Acad. Sci. USA* 96, 13409–13414 (1999). [PubMed: 10557334]
26. Sason H et al. Asc-1 transporter regulation of synaptic activity via the tonic release of D-serine in the forebrain. *Cereb. Cortex* 27, 1573–1587 (2017). [PubMed: 26796213]
27. Ivanov AD & Mothet J-P The plastic D-serine signaling pathway: sliding from neurons to glia and vice-versa. *Neurosci. Lett* 689, 21–25 (2019). [PubMed: 29852209]
28. Foltyn VN et al. Serine racemase modulates intracellular D-serine levels through an  $\alpha,\beta$ -elimination activity. *J. Biol. Chem* 280, 1754–1763 (2005). [PubMed: 15536068]
29. Schell MJ, Molliver ME & Snyder SH D-Serine, an endogenous synaptic modulator: localization to astrocytes and glutamate-stimulated release. *Proc. Natl Acad. Sci. USA* 92, 3948–3952 (1995). [PubMed: 7732010]
30. Perez EJ et al. Enhanced astrocytic D-serine underlies synaptic damage after traumatic brain injury. *J. Clin. Invest* 127, 3114–3125 (2017). [PubMed: 28714867]
31. Tapanes SA et al. Inhibition of glial D-serine release rescues synaptic damage after brain injury. *Glia* 70, 1133–1152 (2022). [PubMed: 35195906]
32. Mustafa AK et al. Serine racemase deletion protects against cerebral ischemia and excitotoxicity. *J. Neurosci. Res* 30, 1413–1416 (2010).
33. Bendikov I et al. A CSF and postmortem brain study of D-serine metabolic parameters in schizophrenia. *Schizophr. Res* 90, 41–51 (2007). [PubMed: 17156977]
34. Wolosker H & Balu DT D-Serine as the gatekeeper of NMDA receptor activity: implications for the pharmacologic management of anxiety disorders. *Transl. Psychiatry* 10, 1–10 (2020). [PubMed: 32066695]
35. Klätte K et al. Impaired D-serine-mediated cotransmission mediates cognitive dysfunction in epilepsy. *J. Neurosci. Res* 33, 13066–13080 (2013).
36. Beesley S et al. D-Serine mitigates cell loss associated with temporal lobe epilepsy. *Nat. Commun* 11, 4966 (2020). [PubMed: 33009404]
37. Mitchell J et al. Familial amyotrophic lateral sclerosis is associated with a mutation in D-amino acid oxidase. *Proc. Natl Acad. Sci USA* 107, 7556–7561 (2010). [PubMed: 20368421]
38. Sasabe J et al. D-Amino acid oxidase controls motoneuron degeneration through D-serine. *Proc. Natl Acad. Sci. USA* 109, 627–632 (2012). [PubMed: 22203986]
39. Spasova K & Föhling M D-Serine — A Useful Biomarker for Renal Injury? (Wiley, 2020).
40. Hamase K, Morikawa A & Zaitsev K D-Amino acids in mammals and their diagnostic value. *J. Chromatogr. B* 781, 73–91 (2002).
41. Johnson CH, Ivanisevic J & Siuzdak G Metabolomics: beyond biomarkers and towards mechanisms. *Nat. Rev. Mol. Cell Biol* 17, 451–459 (2016). [PubMed: 26979502]
42. Schrimpe-Rutledge AC, Codreanu SG, Sherrod SD & McLean JA Untargeted metabolomics strategies — challenges and emerging directions. *J. Am. Soc. Mass Spectrom* 27, 1897–1905 (2016). [PubMed: 27624161]
43. Armstrong D Analysis of D-amino acids: relevance in human disease. *LC GC N. Am* 40, 356–360 (2022).
44. Murtas G & Pollegioni L D-Amino acids as novel blood-based biomarkers. *Curr. Med. Chem* 29, 4202–4215 (2022). [PubMed: 34823459]

45. Paoletti P, Bellone C & Zhou Q NMDA receptor subunit diversity: impact on receptor properties, synaptic plasticity and disease. *Nat. Rev. Neurosci* 14, 383–400 (2013). [PubMed: 23686171]
46. Hansen KB et al. Structure, function, and allosteric modulation of NMDA receptors. *J. Gen. Physiol* 150, 1081–1105 (2018). [PubMed: 30037851]
47. Fuchs SA, Berger R, Klomp LW & De Koning TJ D-Amino acids in the central nervous system in health and disease. *Mol. Genet. Metab* 85, 168–180 (2005). [PubMed: 15979028]
48. Wong JM et al. Postsynaptic serine racemase regulates NMDA receptor function. *J. Neurosci* 40, 9564–9575 (2020). [PubMed: 33158959]
49. Balu DT et al. Serine racemase and D-serine in the amygdala are dynamically involved in fear learning. *Biol. Psychiatry* 83, 273–283 (2018). [PubMed: 29025687]
50. Balu DT et al. Multiple risk pathways for schizophrenia converge in serine racemase knockout mice, a mouse model of NMDA receptor hypofunction. *Proc. Natl Acad. Sci. USA* 110, E2400–E2409 (2013). [PubMed: 23729812]
51. Basu AC et al. Targeted disruption of serine racemase affects glutamatergic neurotransmission and behavior. *Mol. Psychiatry* 14, 719–727 (2009). [PubMed: 19065142]
52. Shleper M, Kartvelishvily E & Wolosker H D-Serine is the dominant endogenous coagonist for NMDA receptor neurotoxicity in organotypic hippocampal slices. *J. Neurosci* 25, 9413–9417 (2005). [PubMed: 16221850]
53. Katsuki H, Nonaka M, Shirakawa H, Kume T & Akaike A Endogenous D-serine is involved in induction of neuronal death by *N*-methyl-D-aspartate and simulated ischemia in rat cerebrocortical slices. *J. Pharmacol. Exp. Ther* 311, 836–844 (2004). [PubMed: 15240826]
54. Piubelli L, Murtas G, Rabattoni V & Pollegioni L The role of D-amino acids in Alzheimer's disease. *J. Alzheimers Dis* 80, 475–492 (2021). [PubMed: 33554911]
55. Ghatak S, Talantova M, McKercher SR & Lipton SA Novel therapeutic approach for excitatory/inhibitory imbalance in neurodevelopmental and neurodegenerative diseases. *Annu. Rev. Pharmacol. Toxicol* 61, 701–721 (2021). [PubMed: 32997602]
56. Hashimoto K et al. Decreased serum levels of D-serine in patients with schizophrenia: evidence in support of the *N*-methyl-D-aspartate receptor hypofunction hypothesis of schizophrenia. *Arch. Gen. Psychiatry* 60, 572–576 (2003). [PubMed: 12796220]
57. Mothet J et al. A critical role for the glial-derived neuromodulator D-serine in the age-related deficits of cellular mechanisms of learning and memory. *Aging Cell* 5, 267–274 (2006). [PubMed: 16842499]
58. Turpin F et al. Reduced serine racemase expression contributes to age-related deficits in hippocampal cognitive function. *Neurobiol. Aging* 32, 1495–1504 (2011). [PubMed: 19800712]
59. Orzylowski M, Fujiwara E, Mousseau DD & Baker GB An overview of the involvement of D-serine in cognitive impairment in normal aging and dementia. *Front. Psychiatry* 12, 754032 (2021). [PubMed: 34707525]
60. Van der Crabben S et al. An update on serine deficiency disorders. *J. Inherit. Metab. Dis* 36, 613–619 (2013). [PubMed: 23463425]
61. Kantrowitz JT et al. Neurophysiological mechanisms of cortical plasticity impairments in schizophrenia and modulation by the NMDA receptor agonist D-serine. *Brain* 139, 3281–3295 (2016). [PubMed: 27913408]
62. Kantrowitz JT et al. D-Serine for the treatment of negative symptoms in individuals at clinical high risk of schizophrenia: a pilot, double-blind, placebo-controlled, randomised parallel group mechanistic proof-of-concept trial. *Lancet Psychiatry* 2, 403–412 (2015). [PubMed: 26360284]
63. Kantrowitz JT et al. Improvement in mismatch negativity generation during D-serine treatment in schizophrenia: correlation with symptoms. *Schizophr. Res* 191, 70–79 (2018). [PubMed: 28318835]
64. Bado P et al. Effects of low-dose D-serine on recognition and working memory in mice. *Psychopharmacology* 218, 461–470 (2011). [PubMed: 21556803]
65. Panizzutti R et al. Association between increased serum D-serine and cognitive gains induced by intensive cognitive training in schizophrenia. *Schizophr. Res* 207, 63–69 (2019). [PubMed: 29699895]



66. Tsai G, Yang P, Chung L-C, Lange N & Coyle JT D-Serine added to antipsychotics for the treatment of schizophrenia. *Biol. Psychiatry* 44, 1081–1089 (1998). [PubMed: 9836012]
67. Heresco-Levy U et al. Pilot controlled trial of D-serine for the treatment of post-traumatic stress disorder. *Int. J. Neuropsychopharmacol* 12, 1275–1282 (2009). [PubMed: 19366490]
68. Moaddel R et al. D-Serine plasma concentration is a potential biomarker of (*R,S*)-ketamine antidepressant response in subjects with treatment-resistant depression. *Psychopharmacology* 232, 399–409 (2015). [PubMed: 25056852]
69. Nava-Gómez L et al. Aging-associated cognitive decline is reversed by D-serine supplementation. *eNeuro* 10.1523/ENEURO.0176-22.2022 (2022).
70. Madeira C et al. D-Serine levels in Alzheimer's disease: implications for novel biomarker development. *Transl. Psychiatry* 5, e561 (2015). [PubMed: 25942042]
71. Biemans EA et al. CSF D-serine concentrations are similar in Alzheimer's disease, other dementias, and elderly controls. *Neurobiol. Aging* 42, 213–216 (2016). [PubMed: 27143438]
72. Piubelli L et al. Serum D-serine levels are altered in early phases of Alzheimer's disease: towards a precocious biomarker. *Transl. Psychiatry* 11, 77 (2021). [PubMed: 33500383]
73. Ito T et al. Serine racemase is involved in D-aspartate biosynthesis. *J. Biochem* 160, 345–353 (2016). [PubMed: 27387750]
74. Wolosker H, D'Aniello A & Snyder S D-Aspartate disposition in neuronal and endocrine tissues: ontogeny, biosynthesis and release. *Neuroscience* 100, 183–189 (2000). [PubMed: 10996468]
75. Schell MJ, Cooper OB & Snyder SH D-Aspartate localizations imply neuronal and neuroendocrine roles. *Proc. Natl Acad. Sci. USA* 94, 2013–2018 (1997). [PubMed: 9050896]
76. Ota N, Shi T & Sweedler JV D-Aspartate acts as a signaling molecule in nervous and neuroendocrine systems. *Amino Acids* 43, 1873–1886 (2012). [PubMed: 22872108]
77. De Rosa A et al. Prenatal expression of D-aspartate oxidase causes early cerebral D-aspartate depletion and influences brain morphology and cognitive functions at adulthood. *Amino Acids* 52, 597–617 (2020). [PubMed: 32185508]
78. Nuzzo T et al. Decreased free D-aspartate levels are linked to enhanced D-aspartate oxidase activity in the dorsolateral prefrontal cortex of schizophrenia patients. *NPJ Schizophr* 3, 16 (2017). [PubMed: 28560262]
79. Errico F et al. Decreased levels of D-aspartate and NMDA in the prefrontal cortex and striatum of patients with schizophrenia. *J. Psychiatr. Res* 47, 1432–1437 (2013). [PubMed: 23835041]
80. Coyle JT Schizophrenia: basic and clinical. *Neurodegener. Dis* 15, 255–280 (2017).
81. Nuzzo T et al. The levels of the NMDA receptor co-agonist D-serine are reduced in the substantia nigra of MPTP-lesioned macaques and in the cerebrospinal fluid of Parkinson's disease patients. *Sci. Rep* 9, 8898 (2019). [PubMed: 31222058]
82. Morikawa A et al. Determination of free D-aspartic acid, D-serine and D-alanine in the brain of mutant mice lacking D-amino-acid oxidase activity. *J. Chromatogr. B* 757, 119–125 (2001).
83. Tsai GE, Yang P, Chang YC & Chong MY D-Alanine added to antipsychotics for the treatment of schizophrenia. *Biol. Psychiatry* 59, 230–234 (2006). [PubMed: 16154544]
84. Fisher GH et al. Free D-aspartate and D-alanine in normal and Alzheimer brain. *Brain Res. Bull* 26, 983–985 (1991). [PubMed: 1933416]
85. Xing Y, Li X, Guo X & Cui Y Simultaneous determination of 18 D-amino acids in rat plasma by an ultrahigh-performance liquid chromatography–tandem mass spectrometry method: application to explore the potential relationship between Alzheimer's disease and D-amino acid level alterations. *Anal. Bioanal. Chem* 408, 141–150 (2016). [PubMed: 26497841]
86. Semenza ER et al. D-Cysteine is an endogenous regulator of neural progenitor cell dynamics in the mammalian brain. *Proc. Natl Acad. Sci. USA* 118, e2110610118 (2021). [PubMed: 34556581]
87. Hofmann GF et al. Neurological manifestations of organic acid disorders. *Eur. J. Pediatr* 153, S94–S100 (1994). [PubMed: 7957396]
88. Achouri Y et al. Identification of a dehydrogenase acting on D-2-hydroxyglutarate. *Biochem. J* 381, 35–42 (2004). [PubMed: 15070399]
89. Junqueira D et al. In vitro effects of D-2-hydroxyglutaric acid on glutamate binding, uptake and release in cerebral cortex of rats. *J. Neurol. Sci* 217, 189–194 (2004). [PubMed: 14706223]

90. Kolker S et al. NMDA receptor activation and respiratory chain complex V inhibition contribute to neurodegeneration in D-2-hydroxyglutaric aciduria. *Eur. J. Neurosci* 16, 21–28 (2002). [PubMed: 12153528]
91. Muntau AC et al. Combined D-2-and L-2-hydroxyglutaric aciduria with neonatal onset encephalopathy: a third biochemical variant of 2-hydroxyglutaric aciduria? *Neuropediatrics* 31, 137–140 (2000). [PubMed: 10963100]
92. Stevens LA, Coresh J, Greene T & Levey AS Assessing kidney function — measured and estimated glomerular filtration rate. *N. Engl. J. Med* 354, 2473–2483 (2006). [PubMed: 16760447]
93. Kimura T, Hesaka A & Isaka Y D-Amino acids and kidney diseases. *Clin. Exp. Nephrol* 24, 404–410 (2020). [PubMed: 32112266]
94. Silbernagl S, Völker K & Dantzer WH D-Serine is reabsorbed in rat renal pars recta. *Am. J. Physiol* 276, F857–F863 (1999). [PubMed: 10362774]
95. Okushima H et al. Intra-body dynamics of D-serine reflects the origin of kidney diseases. *Clin. Exp. Nephrol* 25, 893–901 (2021). [PubMed: 33768329]
96. Iwakawa H, Makabe S, Ito T, Yoshimura T & Watanabe H Urinary D-serine level as a predictive biomarker for deterioration of renal function in patients with atherosclerotic risk factors. *Biomarkers* 24, 159–165 (2019). [PubMed: 30252501]
97. Kawamura M et al. Measurement of glomerular filtration rate using endogenous D-serine clearance in living kidney transplant donors and recipients. *EclinicalMedicine* 43, 101223 (2022). [PubMed: 34934934]
98. Hesaka A et al. D-Serine reflects kidney function and diseases. *Sci. Rep* 9, 5104 (2019). [PubMed: 30911057]
99. Sasabe J et al. Ischemic acute kidney injury perturbs homeostasis of serine enantiomers in the body fluid in mice: early detection of renal dysfunction using the ratio of serine enantiomers. *PLoS ONE* 9, e86504 (2014). [PubMed: 24489731]
100. Young G, Kendall S & Brownjohn A D-Amino acids in chronic renal failure and the effects of dialysis and urinary losses. *Amino Acids* 6, 283–293 (1994). [PubMed: 24189736]
101. Min JZ et al. Determination of dl-amino acids, derivatized with *R*(–)-4-(3-isothiocyanatopyrrolidin-1-yl)-7-(*N,N*-dimethylaminosulfonyl)-2,1,3-benzoxadiazole, in nail of diabetic patients by UPLC–ESI–TOF-MS. *J. Chromatogr. B* 879, 3220–3228 (2011).
102. Lorenzo MP et al. Optimization and validation of a chiral GC-MS method for the determination of free D-amino acids ratio in human urine: application to a gestational diabetes mellitus study. *J. Pharm. Biomed. Anal* 107, 480–487 (2015). [PubMed: 25679092]
103. Canfora EE, Meex RCR, Venema K & Blaak EE Gut microbial metabolites in obesity, NAFLD and T2DM. *Nat. Rev. Endocrinol* 15, 261–273 (2019). [PubMed: 30670819]
104. Cheng Q-Y et al. Sensitive determination of onco-metabolites of D- and L-2-hydroxyglutarate enantiomers by chiral derivatization combined with liquid chromatography/mass spectrometry analysis. *Sci. Rep* 5, 1–11 (2015).
105. Lu J et al. Closing the anion gap: contribution of D-lactate to diabetic ketoacidosis. *Clin. Chim. Acta* 412, 286–291 (2011). [PubMed: 21036159]
106. Ma S et al. D-2-Hydroxyglutarate is essential for maintaining oncogenic property of mutant IDH-containing cancer cells but dispensable for cell growth. *Oncotarget* 6, 8606–8620 (2015). [PubMed: 25825982]
107. Struys EA, Gibson KM & Jakobs C Novel insights into L-2-hydroxyglutaric aciduria: mass isotopomer studies reveal 2-oxoglutaric acid as the metabolic precursor of L-2-hydroxyglutaric acid. *J. Inher. Metab. Dis* 30, 690–693 (2007). [PubMed: 17876720]
108. Ye D, Guan KL & Xiong Y Metabolism, activity, and targeting of D- and L-2-hydroxyglutarates. *Trends Cancer* 4, 151–165 (2018). [PubMed: 29458964]
109. Baek J & Pennathur S Urinary 2-hydroxyglutarate enantiomers are markedly elevated in a murine model of type 2 diabetic kidney disease. *Metabolites* 11, 469 (2021). [PubMed: 34436410]
110. Bastings J, van Eijk HM, Olde Damink SW & Rensen SS D-Amino acids in health and disease: a focus on cancer. *Nutrients* 11, 2205 (2019). [PubMed: 31547425]
111. Nagata Y et al. High concentrations of D-amino acids in human gastric juice. *Amino Acids* 32, 137–140 (2007). [PubMed: 16583309]

112. Han M et al. Development and validation of a rapid, selective, and sensitive LC–MS/MS method for simultaneous determination of D- and L-amino acids in human serum: application to the study of hepatocellular carcinoma. *Anal. Bioanal. Chem* 410, 2517–2531 (2018). [PubMed: 29492623]
113. Du S et al. Altered profiles and metabolism of L- and D-amino acids in cultured human breast cancer cells vs. non-tumorigenic human breast epithelial cells. *J. Pharm. Biomed. Anal* 164, 421–429 (2019). [PubMed: 30445355]
114. Ohshima K et al. Serine racemase enhances growth of colorectal cancer by producing pyruvate from serine. *Nat. Metab* 2, 81–96 (2020). [PubMed: 32694681]
115. Cui Z et al. Integrated bioinformatics analysis of serine racemase as an independent prognostic biomarker in endometrial cancer. *Front. Genet* 13, 906291 (2022). [PubMed: 35923695]
116. Broer A, Rahimi F & Broer S Deletion of amino acid transporter ASCT2 (SLC1A5) reveals an essential role for transporters SNAT1 (SLC38A1) and SNAT2 (SLC38A2) to sustain glutaminolysis in cancer cells. *J. Biol. Chem* 291, 13194–13205 (2016). [PubMed: 27129276]
117. Bodner O et al. D-Serine signaling and NMDAR-mediated synaptic plasticity are regulated by system A-type of glutamine/d-serine dual transporters. *J. Neurosci* 40, 6489–6502 (2020). [PubMed: 32661027]
118. Kaplan E et al. ASCT1 (Slc1a4) transporter is a physiologic regulator of brain D-serine and neurodevelopment. *Proc. Natl Acad. Sci. USA* 115, 9628–9633 (2018). [PubMed: 30185558]
119. Shibuya N et al. A novel pathway for the production of hydrogen sulfide from D-cysteine in mammalian cells. *Nat. Commun* 4, 1366 (2013). [PubMed: 23340406]
120. Hellmich MR & Szabo C *Hydrogen Sulfide and Cancer* (Springer, 2015).
121. El Sayed SM et al. D-Amino acid oxidase-induced oxidative stress, 3-bromopyruvate and citrate inhibit angiogenesis, exhibiting potent anticancer effects. *J. Bioenerg. Biomembr* 44, 513–523 (2012). [PubMed: 22802136]
122. Pollegioni L, Sacchi S & Murtas G Human D-amino acid oxidase: structure, function, and regulation. *Front. Mol. Biosci* 5, 107 (2018). [PubMed: 30547037]
123. North WG, Gao G, Memoli VA, Pang RH & Lynch L Breast cancer expresses functional NMDA receptors. *Breast Cancer Res. Treat* 122, 307–314 (2010). [PubMed: 19784770]
124. Deutsch SI, Tang AH, Burket JA & Benson AD NMDA receptors on the surface of cancer cells: target for chemotherapy? *Biomed. Pharmacother* 68, 493–496 (2014). [PubMed: 24751001]
125. Hogan-Cann AD & Anderson CM Physiological roles of non-neuronal NMDA receptors. *Trends Pharmacol. Sci* 37, 750–767 (2016). [PubMed: 27338838]
126. Du S et al. Roles of N-methyl-D-aspartate receptors and D-amino acids in cancer cell viability. *Mol. Biol. Rep* 47, 6749–6758 (2020). [PubMed: 32892308]
127. Szabo C & Hellmich MR Endogenously produced hydrogen sulfide supports tumor cell growth and proliferation. *Cell Cycle* 12, 2915–2916 (2013). [PubMed: 23974103]
128. Szabo C et al. Tumor-derived hydrogen sulfide, produced by cystathionine- $\beta$ -synthase, stimulates bioenergetics, cell proliferation, and angiogenesis in colon cancer. *Proc. Natl Acad. Sci. USA* 110, 12474–12479 (2013). [PubMed: 23836652]
129. Dang L et al. Cancer-associated IDH1 mutations produce 2-hydroxyglutarate. *Nature* 462, 739–744 (2009). [PubMed: 19935646]
130. Intlekofer AM et al. Hypoxia induces production of L-2-hydroxyglutarate. *Cell Metab* 22, 304–311 (2015). [PubMed: 26212717]
131. Yang H, Ye D, Guan KL & Xiong Y IDH1 and IDH2 mutations in tumorigenesis: mechanistic insights and clinical perspectives. *Clin. Cancer Res* 18, 5562–5571 (2012). [PubMed: 23071358]
132. Wang P et al. Oncometabolite D-2-hydroxyglutarate inhibits ALKBH DNA repair enzymes and sensitizes IDH mutant cells to alkylating agents. *Cell Rep* 13, 2353–2361 (2015). [PubMed: 26686626]
133. Xu W et al. Oncometabolite 2-hydroxyglutarate is a competitive inhibitor of  $\alpha$ -ketoglutarate-dependent dioxygenases. *Cancer Cell* 19, 17–30 (2011). [PubMed: 21251613]
134. Brückner H & Schieber A Determination of amino acid enantiomers in human urine and blood serum by gas chromatography–mass spectrometry. *Biomed. Chromatogr* 15, 166–172 (2001). [PubMed: 11391672]

135. Wolfender J-L, Marti G, Thomas A & Bertrand S Current approaches and challenges for the metabolite profiling of complex natural extracts. *J. Chromatogr. A* 1382, 136–164 (2015). [PubMed: 25464997]
136. Mochizuki T et al. Towards the chiral metabolomics: liquid chromatography–mass spectrometry based dl-amino acid analysis after labeling with a new chiral reagent, (*S*)-2, 5-dioxopyrrolidin-1-yl-1-(4,6-dimethoxy-1, 3, 5-triazin-2-yl) pyrrolidine-2-carboxylate, and the application to saliva of healthy volunteers. *Anal. Chim. Acta* 875, 73–82 (2015). [PubMed: 25937108]
137. Szök É, Vincze I & Tábi T Chiral separations for D-amino acid analysis in biological samples. *J. Pharm. Biomed. Anal* 130, 100–109 (2016). [PubMed: 27435607]
138. Cavazzini A, Pasti L, Massi A, Marchetti N & Dondi F Recent applications in chiral high performance liquid chromatography: a review. *Anal. Chim. Acta* 706, 205–222 (2011). [PubMed: 22023854]
139. Grossman PD & Colburn JC *Capillary Electrophoresis: Theory and Practice* (Academic, 2012).
140. Ramautar R, Berger R, van der Greef J & Hankemeier T Human metabolomics: strategies to understand biology. *Curr. Opin. Chem. Biol* 17, 841–846 (2013). [PubMed: 23849548]
141. Scalbert A et al. Mass-spectrometry-based metabolomics: limitations and recommendations for future progress with particular focus on nutrition research. *Metabolomics* 5, 435–458 (2009). [PubMed: 20046865]
142. Lloyd DK & Goodall DM Polarimetric detection in high-performance liquid chromatography. *Chirality* 1, 251–264 (1989). [PubMed: 2701852]
143. Purvinis G, Cameron BD & Altrogge DM Noninvasive polarimetric-based glucose monitoring: an in vivo study. *J. Diabetes Sci. Technol* 5, 380–387 (2011). [PubMed: 21527109]
144. Borovkova M et al. Evaluating  $\beta$ -amyloidosis progression in Alzheimer's disease with Mueller polarimetry. *Biomed. Opt. Express* 11, 4509–4519 (2020). [PubMed: 32923060]
145. Greenfield NJ Using circular dichroism spectra to estimate protein secondary structure. *Nat. Protoc* 1, 2876–2890 (2006). [PubMed: 17406547]
146. Keller BO, Sui J, Young AB & Whittall RM Interferences and contaminants encountered in modern mass spectrometry. *Anal. Chim. Acta* 627, 71–81 (2008). [PubMed: 18790129]
147. Wu L & Han DK Overcoming the dynamic range problem in mass spectrometry-based shotgun proteomics. *Expert Rev. Proteom* 3, 611–619 (2006).
148. Dettmer K, Aronov PA & Hammock BD Mass spectrometry-based metabolomics. *Mass Spectrom. Rev* 26, 51–78 (2007). [PubMed: 16921475]
149. Vuckovic D Current trends and challenges in sample preparation for global metabolomics using liquid chromatography–mass spectrometry. *Anal. Bioanal. Chem* 403, 1523–1548 (2012). [PubMed: 22576654]
150. Doherty CM & Forbes RB Diagnostic lumbar puncture. *Ulster Med. J* 83, 93 (2014).
151. Lewis SM & Tatsumi N in *Dacie Lewis Pr. Hematol* 10th edn Ch. 1 (Elsevier, 2006).
152. Gübitz G & Schmid MG Chiral separation by chromatographic and electromigration techniques: a review. *Biopharm. Drug Dispos* 22, 291–336 (2001). [PubMed: 11835252]
153. Ang JE et al. Identification of human plasma metabolites exhibiting time-of-day variation using an untargeted liquid chromatography–mass spectrometry metabolomic approach. *Chronobiol. Int* 29, 868–881 (2012). [PubMed: 22823870]
154. Kim K et al. Mealtime, temporal, and daily variability of the human urinary and plasma metabolomes in a tightly controlled environment. *PLoS ONE* 9, e86223 (2014). [PubMed: 24475090]
155. Lin C-H, Yang H-T & Lane H-Y D-Glutamate, D-serine, and D-alanine differ in their roles in cognitive decline in patients with Alzheimer's disease or mild cognitive impairment. *Pharmacol. Biochem. Behav* 185, 172760 (2019). [PubMed: 31422081]
156. Armstrong DW, Kullman JP, Chen X & Rowe M Composition and chirality of amino acids in aerosol/dust from laboratory and residential enclosures. *Chirality* 13, 153–158 (2001). [PubMed: 11270325]
157. Yin P, Lehmann R & Xu G Effects of pre-analytical processes on blood samples used in metabolomics studies. *Anal. Bioanal. Chem* 407, 4879–4892 (2015). [PubMed: 25736245]

158. Khadka M et al. The effect of anticoagulants, temperature, and time on the human plasma metabolome and lipidome from healthy donors as determined by liquid chromatography–mass spectrometry. *Biomolecules* 9, 200 (2019). [PubMed: 31126114]
159. Pedersen-Bjergaard S & Rasmussen KE Liquid–liquid–liquid microextraction for sample preparation of biological fluids prior to capillary electrophoresis. *Anal. Chem* 71, 2650–2656 (1999). [PubMed: 10424162]
160. Nagata Y, Akino T & Ohno K Microdetermination of serum D-amino acids. *Anal. Chem* 150, 238–242 (1985).
161. Brückner H & Hausch M Gas chromatographic characterization of free D-amino acids in the blood serum of patients with renal disorders and of healthy volunteers. *J. Chromatogr. B* 614, 7–17 (1993).
162. Lesche D et al. Does centrifugation matter? Centrifugal force and spinning time alter the plasma metabolome. *Metabolomics* 12, 159 (2016). [PubMed: 27729833]
163. Jobard E et al. A systematic evaluation of blood serum and plasma pre-analytics for metabolomics cohort studies. *Int. J. Mol. Sci* 17, 2035 (2016). [PubMed: 27929400]
164. Heireman L et al. Causes, consequences and management of sample hemolysis in the clinical laboratory. *Clin. Biochem* 50, 1317–1322 (2017). [PubMed: 28947321]
165. Jiang L, He L & Fountoulakis M Comparison of protein precipitation methods for sample preparation prior to proteomic analysis. *J. Chromatogr. A* 1023, 317–320 (2004). [PubMed: 14753699]
166. Pätzold R, Schieber A & Brückner H Gas chromatographic quantification of free D-amino acids in higher vertebrates. *Biomed. Chromatogr* 19, 466–473 (2005). [PubMed: 16037932]
167. Patti GJ Separation strategies for untargeted metabolomics. *J. Sep. Sci* 34, 3460–3469 (2011). [PubMed: 21972197]
168. Yu Z et al. Differences between human plasma and serum metabolite profiles. *PLoS ONE* 6, e21230 (2011). [PubMed: 21760889]
169. Teahan O et al. Impact of analytical bias in metabolomic studies of human blood serum and plasma. *Anal. Chem* 78, 4307–4318 (2006). [PubMed: 16808437]
170. Asakura S & Konno R Origin of D-serine present in urine of mutant mice lacking D-amino-acid oxidase activity. *Amino Acids* 12, 213–223 (1997).
171. Kato S, Kito Y, Hemmi H & Yoshimura T Simultaneous determination of D-amino acids by the coupling method of D-amino acid oxidase with high-performance liquid chromatography. *J. Chromatogr. B* 879, 3190–3195 (2011).
172. Nagata Y et al. The presence of high concentrations of free D-amino acids in human saliva. *Life Sci* 78, 1677–1681 (2006). [PubMed: 16480744]
173. Römisch-Margl W et al. Procedure for tissue sample preparation and metabolite extraction for high-throughput targeted metabolomics. *Metabolomics* 8, 133–142 (2012).
174. González-Domínguez R, González-Domínguez Á, Sayago A & Fernández-Recamales Á Recommendations and best practices for standardizing the pre-analytical processing of blood and urine samples in metabolomics. *Metabolites* 10, 229 (2020). [PubMed: 32503183]
175. Stevens VL, Hoover E, Wang Y & Zanetti KA Pre-analytical factors that affect metabolite stability in human urine, plasma, and serum: a review. *Metabolites* 9, 156 (2019). [PubMed: 31349624]
176. Cajka T & Fiehn O Toward merging untargeted and targeted methods in mass spectrometry-based metabolomics and lipidomics. *Anal. Chem* 88, 524–545 (2016). [PubMed: 26637011]
177. Berthod A *Chiral Recognition in Separation Methods* (Springer, 2010).
178. Subramanian G *Chiral Separation Techniques: A Practical Approach* (Wiley, 2008).
179. Aswad DW Determination of D- and L-aspartate in amino acid mixtures by high-performance liquid chromatography after derivatization with a chiral adduct of *o*-phthalaldehyde. *Anal. Biochem* 137, 405–409 (1984). [PubMed: 6731824]
180. Fisher G et al. Free D- and L-amino acids in ventricular cerebrospinal fluid from Alzheimer and normal subjects. *Amino Acids* 15, 263–269 (1998). [PubMed: 9871505]

181. Gibson K et al. Stable-isotope dilution analysis of D- and L-2-hydroxyglutaric acid: application to the detection and prenatal diagnosis of D- and L-2-hydroxyglutaric acidemias. *Pediatr. Res* 34, 277–280 (1993). [PubMed: 8134166]
182. El Zahar NM, Magdy N, El-Kosasy AM & Bartlett MG Chromatographic approaches for the characterization and quality control of therapeutic oligonucleotide impurities. *Biomed. Chromatogr* 32, e4088 (2018).
183. Kagan H & Fiaud J Kinetic resolution. *Top. Stereochem* 18, 249–330 (1988).
184. Rashed MS, AlAmoudi M & Aboul-Enein HY Chiral liquid chromatography tandem mass spectrometry in the determination of the configuration of 2-hydroxyglutaric acid in urine. *Biomed. Chromatogr* 14, 317–320 (2000). [PubMed: 10960831]
185. Kimura T et al. Chiral amino acid metabolomics for novel biomarker screening in the prognosis of chronic kidney disease. *Sci. Rep* 6, 26137 (2016). [PubMed: 27188851]
186. Furusho A et al. Three-dimensional high-performance liquid chromatographic determination of Asn, Ser, Ala, and Pro enantiomers in the plasma of patients with chronic kidney disease. *Anal. Chem* 91, 11569–11575 (2019). [PubMed: 31436409]
187. Du S, Wang Y, Weatherly CA, Holden K & Armstrong DW Variations of L- and D-amino acid levels in the brain of wild-type and mutant mice lacking D-amino acid oxidase activity. *Anal. Bioanal. Chem* 410, 2971–2979 (2018). [PubMed: 29532193]
188. Armstrong D, Duncan J & Lee S Evaluation of D-amino acid levels in human urine and in commercial L-amino acid samples. *Amino Acids* 1, 97–106 (1991). [PubMed: 24194052]
189. McNair HM, Miller JM & Snow NH *Basic Gas Chromatography* (Wiley, 2019).
190. Farajzadeh MA, Nouri N & Khorram P Derivatization and microextraction methods for determination of organic compounds by gas chromatography. *Trends Analyt. Chem* 55, 14–23 (2014).
191. Charissou A, Ait-Ameur L & Birlouez-Aragon I Evaluation of a gas chromatography/mass spectrometry method for the quantification of carboxymethyllysine in food samples. *J. Chromatogr. A* 1140, 189–194 (2007). [PubMed: 17174315]
192. Creamer JS, Mora MF & Willis PA Stability of reagents used for chiral amino acid analysis during spaceflight missions in high-radiation environments. *Electrophoresis* 39, 2864–2871 (2018). [PubMed: 30216482]
193. Bernardo-Bermejo S, Sánchez-López E, Castro-Puyana M & Marina ML Chiral capillary electrophoresis. *Trends Analyt. Chem* 124, 115807 (2020).
194. Li S, Yu Q, Lu X & Zhao S Determination of D,L-serine in midbrain of Parkinson's disease mouse by capillary electrophoresis with in-column light-emitting diode induced fluorescence detection. *J. Sep. Sci* 32, 282–287 (2009). [PubMed: 19156646]
195. Martineau M et al. Storage and uptake of D-serine into astrocytic synaptic-like vesicles specify gliotransmission. *J. Neurosci* 33, 3413–3423 (2013). [PubMed: 23426669]
196. Patel AV, Kawai T, Wang L, Rubakhin SS & Sweedler JV Chiral measurement of aspartate and glutamate in single neurons by large-volume sample stacking capillary electrophoresis. *Anal. Chem* 89, 12375–12382 (2017). [PubMed: 29064231]
197. Fanali C & Fanali S Chiral separations using miniaturized techniques: state of the art and perspectives. *Isr. J. Chem* 56, 958–967 (2016).
198. Merola G, Fu H, Tagliaro F, Macchia T & McCord BR Chiral separation of 12 cathinone analogs by cyclodextrin-assisted capillary electrophoresis with UV and mass spectrometry detection. *Electrophoresis* 35, 3231–3241 (2014). [PubMed: 24947960]
199. Krait S, Konjaria ML & Scriba GK Advances of capillary electrophoresis enantioseparations in pharmaceutical analysis (2017–2020). *Electrophoresis* 42, 1709–1725 (2021). [PubMed: 33433919]
200. Beckonert O et al. Metabolic profiling, metabolomic and metabonomic procedures for NMR spectroscopy of urine, plasma, serum and tissue extracts. *Nat. Protoc* 2, 2692 (2007). [PubMed: 18007604]
201. Suh EH et al. Detection of glucose-derived D- and L-lactate in cancer cells by the use of a chiral NMR shift reagent. *Cancer Metab* 9, 38 (2021). [PubMed: 34742347]

202. Bal D, Gradowska W & Gryf-Keller A Determination of the absolute configuration of 2-hydroxyglutaric acid and 5-oxoproline in urine samples by high-resolution NMR spectroscopy in the presence of chiral lanthanide complexes. *J. Pharm. Biomed. Anal* 28, 1061–1071 (2002). [PubMed: 12049971]
203. Wenzel TJ & Wilcox JD Chiral reagents for the determination of enantiomeric excess and absolute configuration using NMR spectroscopy. *Chirality* 15, 256–270 (2003). [PubMed: 12582993]
204. Emwas A-H et al. NMR spectroscopy for metabolomics research. *Metabolites* 9, 123 (2019). [PubMed: 31252628]
205. Rosini E, D'Antona P & Pollegioni L Biosensors for D-amino acids: detection methods and applications. *Int. J. Mol. Sci* 21, 4574 (2020). [PubMed: 32605078]
206. Trinder P Determination of glucose in blood using glucose oxidase with an alternative oxygen acceptor. *Ann. Clin. Biochem* 6, 24–27 (1969).
207. Zhang Z et al. Non-invasive detection of gastric cancer relevant D-amino acids with luminescent DNA/silver nanoclusters. *Nanoscale* 9, 19367–19373 (2017). [PubMed: 29199749]
208. Mothet JP et al. Glutamate receptor activation triggers a calcium-dependent and SNARE protein-dependent release of the gliotransmitter D-serine. *Proc. Natl Acad. Sci. USA* 102, 5606–5611 (2005). [PubMed: 15800046]
209. Fisher GH et al. Free D-amino acids in human cerebrospinal fluid of Alzheimer disease, multiple sclerosis, and healthy control subjects. *Mol. Chem. Neuropathol* 23, 115–124 (1994). [PubMed: 7702702]
210. Shi R et al. The interaction of K and O<sub>2</sub> on Au(111): multiple growth modes of potassium oxide and their catalytic activity for CO oxidation. *Angew. Chem. Int. Ed* 61, e202208666 (2022).
211. Ma J, Zhang X, Huang X, Luo S & Meggers E Preparation of chiral-at-metal catalysts and their use in asymmetric photoredox chemistry. *Nat. Protoc* 13, 605–632 (2018). [PubMed: 29494576]
212. Shoja Y, Rafati AA & Ghodsi J Enzymatic biosensor based on entrapment of D-amino acid oxidase on gold nanofilm/MWCNTs nanocomposite modified glassy carbon electrode by sol-gel network: analytical applications for D-alanine in human serum. *Enzyme Microb. Technol* 100, 20–27 (2017). [PubMed: 28284308]
213. Nieh C-H, Kitazumi Y, Shirai O & Kano K Sensitive D-amino acid biosensor based on oxidase/peroxidase system mediated by pentacyanoferrate-bound polymer. *Biosens. Bioelectron* 47, 350–355 (2013). [PubMed: 23603133]
214. Rabinovitch B, March W & Adams RL Noninvasive glucose monitoring of the aqueous humor of the eye: part I. Measurement of very small optical rotations. *Diabetes Care* 5, 254–258 (1982). [PubMed: 7172992]
215. Berova N, Nakanishi K & Woody RW *Circular Dichroism: Principles and Applications* (Wiley, 2000).
216. Lecoer-Lorin M, Delepee R, Ribet JP & Morin P Chiral analysis of milnacipran by a nonchiral HPLC–circular dichroism: improvement of the linearity of dichroic response by temperature control. *J. Sep. Sci* 31, 3009–3014 (2008). [PubMed: 18785147]
217. Luo Y et al. A novel potential primary method for quantification of enantiomers by high performance liquid chromatography–circular dichroism. *Sci. Rep* 8, 1–11 (2018). [PubMed: 29311619]
218. Pelton JT & McLean LR Spectroscopic methods for analysis of protein secondary structure. *Anal. Biochem* 277, 167–176 (2000). [PubMed: 10625503]
219. Kypr J, Kejnovska I, Renciuik D & Vorlickova M Circular dichroism and conformational polymorphism of DNA. *Nucleic Acids Res* 37, 1713–1725 (2009). [PubMed: 19190094]
220. Morvan M & Mikšík I Recent advances in chiral analysis of proteins and peptides. *Separations* 8, 112 (2021).
221. Micsonai A et al. Accurate secondary structure prediction and fold recognition for circular dichroism spectroscopy. *Proc. Natl Acad. Sci. USA* 112, E3095–E3103 (2015). [PubMed: 26038575]

222. Kong K, Kendall C, Stone N & Notingher I Raman spectroscopy for medical diagnostics — from in-vitro biofluid assays to in-vivo cancer detection. *Adv. Drug Deliv. Rev* 89, 121–134 (2015). [PubMed: 25809988]
223. Nafie LA Infrared and Raman vibrational optical activity: theoretical and experimental aspects. *Annu. Rev. Phys. Chem* 48, 357–386 (1997). [PubMed: 9348659]
224. Barron LD The development of biomolecular Raman optical activity spectroscopy. *Biomed. Spectrosc. Imaging* 4, 223–253 (2015).
225. Zhu F, Isaacs NW, Hecht L & Barron LD Raman optical activity: a tool for protein structure analysis. *Structure* 13, 1409–1419 (2005). [PubMed: 16216573]
226. Yamamoto S & Bou P Detection of molecular chirality by induced resonance Raman optical activity in europium complexes. *Angew. Chem. Int. Ed* 51, 11058–11061 (2012).
227. Stephens PJ, Devlin FJ & Pan JJ The determination of the absolute configurations of chiral molecules using vibrational circular dichroism (VCD) spectroscopy. *Chirality* 20, 643–663 (2008). [PubMed: 17955495]
228. Guo C et al. Determination of enantiomeric excess in samples of chiral molecules using Fourier transform vibrational circular dichroism spectroscopy: simulation of real-time reaction monitoring. *Anal. Chem* 76, 6956–6966 (2004). [PubMed: 15571347]
229. Armstrong DW, Yu J, Cole HD, McFarland SA & Nafie J Chiral resolution and absolute configuration determination of new metal-based photodynamic therapy antitumor agents. *J. Pharm. Biomed. Anal* 204, 114233 (2021). [PubMed: 34252819]
230. Zhang P & Polavarapu PL Vibrational circular dichroism of matrix-assisted amino acid films in the mid-infrared region. *Appl. Spectrosc* 60, 378–385 (2006). [PubMed: 16613633]
231. Hentschel M, Schaferling M, Duan X, Giessen H & Liu N Chiral plasmonics. *Sci. Adv* 3, e1602735 (2017). [PubMed: 28560336]
232. Solomon ML et al. Nanophotonic platforms for chiral sensing and separation. *Acc. Chem. Res* 53, 588–598 (2020). [PubMed: 31913015]
233. Zhao Y et al. Chirality detection of enantiomers using twisted optical metamaterials. *Nat. Commun* 8, 14180 (2017). [PubMed: 28120825]
234. Wu Z & Zheng Y Moiré chiral metamaterials. *Adv. Opt. Mater* 5, 1700034 (2017).
235. Wu Z & Zheng Y Moiré metamaterials and metasurfaces. *Adv. Opt. Mater* 6, 1701057 (2018).
236. Hendry E et al. Ultrasensitive detection and characterization of biomolecules using superchiral fields. *Nat. Nanotechnol* 5, 783 (2010). [PubMed: 21037572]
237. Liu Y et al. Label-free ultrasensitive detection of abnormal chiral metabolites in diabetes. *ACS Nano* 15, 6448–6456 (2021). [PubMed: 33760602]
238. Wang X & Tang Z Circular dichroism studies on plasmonic nanostructures. *Small* 13, 1601115 (2017).
239. Zhang Q et al. Unraveling the origin of chirality from plasmonic nanoparticle–protein complexes. *Science* 365, 1475–1478 (2019). [PubMed: 31604278]
240. Xu L et al. Highly selective recognition and ultrasensitive quantification of enantiomers. *J. Mater. Chem. B* 1, 4478–4483 (2013). [PubMed: 32261120]
241. Hu J, Lawrence M & Dionne JA High quality factor dielectric metasurfaces for ultraviolet circular dichroism spectroscopy. *ACS Photonics* 7, 36–42 (2019).
242. Lee YY, Kim RM, Im SW, Balamurugan M & Nam KT Plasmonic metamaterials for chiral sensing applications. *Nanoscale* 12, 58–66 (2020). [PubMed: 31815994]
243. Yoo S & Park Q-H Metamaterials and chiral sensing: a review of fundamentals and applications. *Nanophotonics* 8, 249–261 (2019).
244. Paiva-Marques WA, Reyes Gómez F, Oliveira ON & Mejía-Salazar JR Chiral plasmonics and their potential for point-of-care biosensing applications. *Sensors* 20, 944 (2020). [PubMed: 32050725]
245. Abdali S & Blanch EW Surface enhanced Raman optical activity (SEROA). *Chem. Soc. Rev* 37, 980–992 (2008). [PubMed: 18443683]
246. Rocks L et al. Through-space transfer of chiral information mediated by a plasmonic nanomaterial. *Nat. Chem* 7, 591 (2015). [PubMed: 26100808]



247. Mitra S Sample Preparation Techniques in Analytical Chemistry Vol. 237 (Wiley, 2004).
248. Kumar R & Ismail A Fouling control on microfiltration/ultrafiltration membranes: effects of morphology, hydrophilicity, and charge. *J. Appl. Polym. Sci* 132, 42042 (2015).
249. Gilar M, Bouvier ES & Compton BJ Advances in sample preparation in electromigration, chromatographic and mass spectrometric separation methods. *J. Chromatogr. A* 909, 111–135 (2001). [PubMed: 11269513]
250. Goodwin RJ Sample preparation for mass spectrometry imaging: small mistakes can lead to big consequences. *J. Proteom* 75, 4893–4911 (2012).
251. Pusztai L, Hatzis C & Andre F Reproducibility of research and preclinical validation: problems and solutions. *Nat. Rev. Clin. Oncol* 10, 720–724 (2013). [PubMed: 24080600]
252. Addona TA et al. Multi-site assessment of the precision and reproducibility of multiple reaction monitoring–based measurements of proteins in plasma. *Nat. Biotechnol* 27, 633–641 (2009). [PubMed: 19561596]
253. Yager P, Domingo GJ & Gerdes J Point-of-care diagnostics for global health. *Annu. Rev. Biomed. Eng* 10, 107–144 (2008). [PubMed: 18358075]
254. Lippa PB, Müller C, Schlichtiger A & Schlebusch H Point-of-care testing (POCT): current techniques and future perspectives. *Trends Analyt. Chem* 30, 887–898 (2011).
255. National Institute of Biomedical Imaging and Bioengineering/National Heart, Lung, and Blood Institute/National Science Foundation Workshop Faculty, Price CP & Kricka LJ Improving healthcare accessibility through point-of-care technologies. *Clin. Chem* 53, 1665–1675 (2007). [PubMed: 17660275]
256. Gałuszka A, Migaszewski ZM & Namieńnik J Moving your laboratories to the field — advantages and limitations of the use of field portable instruments in environmental sample analysis. *Environ. Res* 140, 593–603 (2015). [PubMed: 26051907]
257. Kuehnbaum NL & Britz-McKibbin P New advances in separation science for metabolomics: resolving chemical diversity in a post-genomic era. *Chem. Rev* 113, 2437–2468 (2013). [PubMed: 23506082]
258. Gowda GN et al. Metabolomics-based methods for early disease diagnostics. *Expert Rev. Mol. Diagn* 8, 617–633 (2008). [PubMed: 18785810]
259. Polavarapu PL *Chiral Analysis: Advances in Spectroscopy, Chromatography and Emerging Methods* (Elsevier, 2018).
260. Newgard CB Metabolomics and metabolic diseases: where do we stand? *Cell Metab* 25, 43–56 (2017). [PubMed: 28094011]
261. Li S et al. Predicting network activity from high throughput metabolomics. *PLoS Comput. Biol* 9, e1003123 (2013). [PubMed: 23861661]
262. van den Berg RA, Hoefsloot HC, Westerhuis JA, Smilde AK & van der Werf MJ Centering, scaling, and transformations: improving the biological information content of metabolomics data. *BMC Genomics* 7, 142 (2006). [PubMed: 16762068]
263. Lalkhen AG & McCluskey A Clinical tests: sensitivity and specificity. *Contin. Educ. Anaesth. Crit. Care Pain* 8, 221–223 (2008).
264. Nie S & Emory SR Probing single molecules and single nanoparticles by surface-enhanced Raman scattering. *Science* 275, 1102–1106 (1997). [PubMed: 9027306]
265. Friedman M & Levin CE Nutritional and medicinal aspects of D-amino acids. *Amino Acids* 42, 1553–1582 (2012). [PubMed: 21519915]
266. Wang Z et al. Quantification of aminobutyric acids and their clinical applications as biomarkers for osteoporosis. *Commun. Biol* 3, 39 (2020). [PubMed: 31969651]
267. Nota B et al. Deficiency in SLC25A1, encoding the mitochondrial citrate carrier, causes combined D-2- and L-2-hydroxyglutaric aciduria. *Am. J. Hum. Genet* 92, 627–631 (2013). [PubMed: 23561848]
268. Strain SK, Groves MD, Olino KL & Emmett MR Measurement of 2-hydroxyglutarate enantiomers in serum by chiral gas chromatography–tandem mass spectrometry and its application as a biomarker for IDH mutant gliomas. *Clin. Mass Spectrom* 15, 16–24 (2020).

269. Willekens C et al. Serum 2-hydroxyglutarate level can predict IDH2 mutation in myeloid sarcoma. *Blood* 126, 3835 (2015).
270. Struys EA et al. Mutations in the D-2-hydroxyglutarate dehydrogenase gene cause D-2-hydroxyglutaric aciduria. *Am. J. Hum. Genet* 76, 358–360 (2005). [PubMed: 15609246]
271. Gibson KM, Craigen W, Herman GE & Jakobs C D-2-Hydroxyglutaric aciduria in a newborn with neurological abnormalities: a new neurometabolic disorder? *J. Inherit. Metab. Dis* 16, 497–500 (1993). [PubMed: 7609436]
272. Rodrigues DGB et al. Experimental evidence of oxidative stress in patients with L-2-hydroxyglutaric aciduria and that L-carnitine attenuates in vitro DNA damage caused by D-2-hydroxyglutaric and L-2-hydroxyglutaric acids. *Toxicol. Vitro* 42, 47–53 (2017).
273. Huang Y, Shi M & Zhao S Quantification of D-Asp and D-Glu in rat brain and human cerebrospinal fluid by microchip electrophoresis. *J. Sep. Sci* 32, 3001–3006 (2009). [PubMed: 19642099]
274. Hashimoto K et al. Possible role of D-serine in the pathophysiology of Alzheimer's disease. *Prog. Neuropsychopharmacol. Biol. Psychiatry* 28, 385–388 (2004). [PubMed: 14751437]
275. Ohnuma T et al. Changes in plasma glycine, L-serine, and D-serine levels in patients with schizophrenia as their clinical symptoms improve: results from the Juntendo University Schizophrenia Projects (JUSP). *Prog. Neuropsychopharmacol. Biol. Psychiatry* 32, 1905–1912 (2008). [PubMed: 18835577]
276. Grant SL, Shulman Y, Tibbo P, Hampson DR & Baker GB Determination of D-serine and related neuroactive amino acids in human plasma by high-performance liquid chromatography with fluorimetric detection. *J. Chromatogr. B* 844, 278–282 (2006).
277. Visser WF et al. A sensitive and simple ultra-high-performance-liquid chromatography–tandem mass spectrometry based method for the quantification of D-amino acids in body fluids. *J. Chromatogr. A* 1218, 7130–7136 (2011). [PubMed: 21890145]
278. Fuchs SA et al. Two mass-spectrometric techniques for quantifying serine enantiomers and glycine in cerebrospinal fluid: potential confounders and age-dependent ranges. *Clin. Chem* 54, 1443–1450 (2008). [PubMed: 18606633]
279. Barbot C et al. L-2-Hydroxyglutaric aciduria: clinical, biochemical and magnetic resonance imaging in six Portuguese pediatric patients. *Brain Dev* 19, 268–273 (1997). [PubMed: 9187477]
280. Topcu M et al. L-2-hydroxyglutaric aciduria: a report of 29 patients. *Turk. J. Pediatr* 47, 1–7 (2005). [PubMed: 15884621]
281. Kranendijk M et al. Development and implementation of a novel assay for L-2-hydroxyglutarate dehydrogenase (L-2-HGDH) in cell lysates: L-2-HGDH deficiency in 15 patients with L-2-hydroxyglutaric aciduria. *J. Inherit. Metab. Dis* 32, 713 (2009). [PubMed: 19821142]
282. Zhao S, Wang B, He M, Bai W & Chen L Determination of free D-alanine in the human plasma by capillary electrophoresis with optical fiber light-emitting diode-induced fluorescence detection. *Anal. Chim. Acta* 569, 182–187 (2006).
283. Scheijen JL et al. L(+) and D(–) lactate are increased in plasma and urine samples of type 2 diabetes as measured by a simultaneous quantification of L(+) and D(–) lactate by reversed-phase liquid chromatography tandem mass spectrometry. *Exp. Diabetes Res* 2012, 234812 (2012). [PubMed: 22474418]
284. Brandt RB, Siegel SA, Waters MG & Bloch MH Spectrophotometric assay for D(–)-lactate in plasma. *Anal. Biochem* 102, 39–46 (1980). [PubMed: 7356162]
285. Tsutsui H et al. Simultaneous determination of dl-lactic acid and dl-3-hydroxybutyric acid enantiomers in saliva of diabetes mellitus patients by high-throughput LC–ESI-MS/MS. *Anal. Bioanal. Chem* 404, 1925–1934 (2012). [PubMed: 22895741]
286. Pandey R et al. Novel strategy for untargeted chiral metabolomics using liquid chromatography–high resolution tandem mass spectrometry. *Anal. Chem* 93, 5805–5814 (2021). [PubMed: 33818082]
287. Takahashi M, Morita M, Niwa O & Tabei H Highly sensitive high-performance liquid chromatography detection of catecholamine with interdigitated array microelectrodes. *J. Electroanal. Chem* 335, 253–263 (1992).

288. Creamer JS, Mora MF & Willis PA Enhanced resolution of chiral amino acids with capillary electrophoresis for biosignature detection in extraterrestrial samples. *Anal. Chem* 89, 1329–1337 (2017). [PubMed: 28194989]
289. Rosini E, D'Antona P & Pollegioni L Biosensors for D-amino acids: detection methods and applications. *Int. J. Mol. Sci* 21, 4574 (2020). [PubMed: 32605078]

Author Manuscript

Author Manuscript

Author Manuscript

Author Manuscript

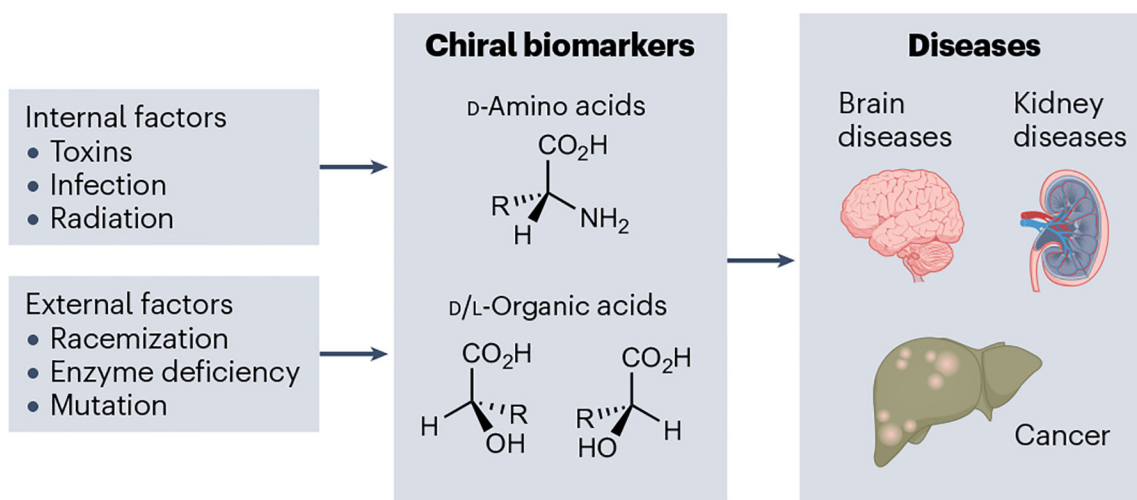


**Fig. 1 |. Influential factors for ‘abnormal’ chirality, common chiral biomarkers and associated diseases.**

Internal and external factors can induce abnormal concentrations of chiral biomarkers in the human body, which are associated with various diseases.

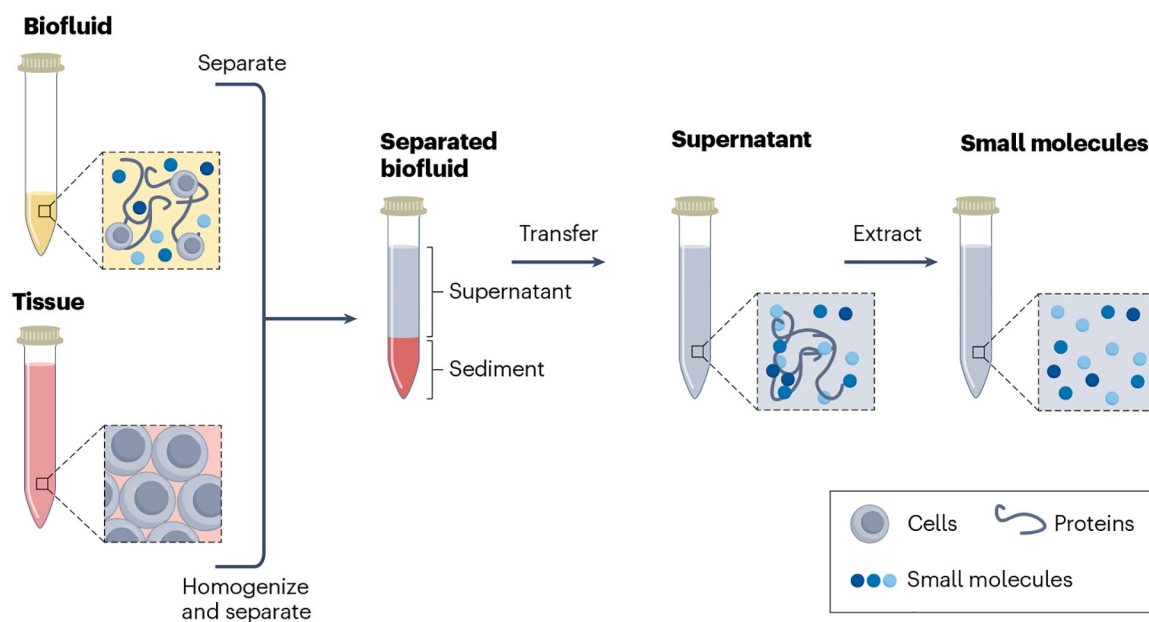


**Fig. 2 |. Sample preparation before chiral detection.**

Filtration and extraction of chiral small molecules from biofluids and tissues.

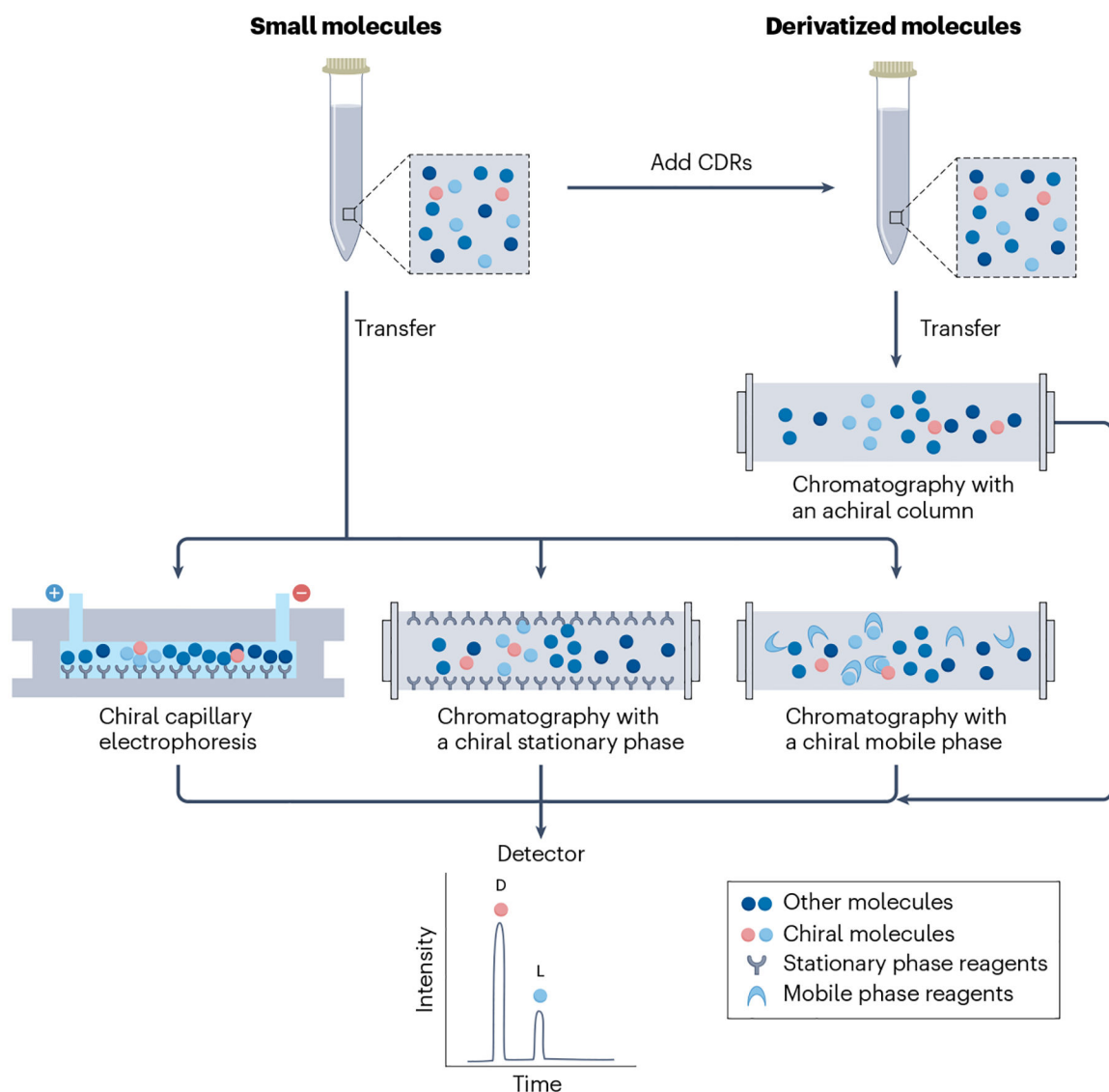


**Fig. 3 | Chiral detection of small molecules via chromatography and capillary electrophoresis coupled to mass spectrometry.**

After sample preparation, small molecules can be enantiomerically separated using a chiral selector, such as a chiral derivatization reagent (CDR), a chiral mobile phase or a chiral stationary phase during chromatography. The small molecules can also be enantioselectively separated using chiral capillary electrophoresis. The enantiomers, which have different retention times, are separated and resolved by mass spectrometry.

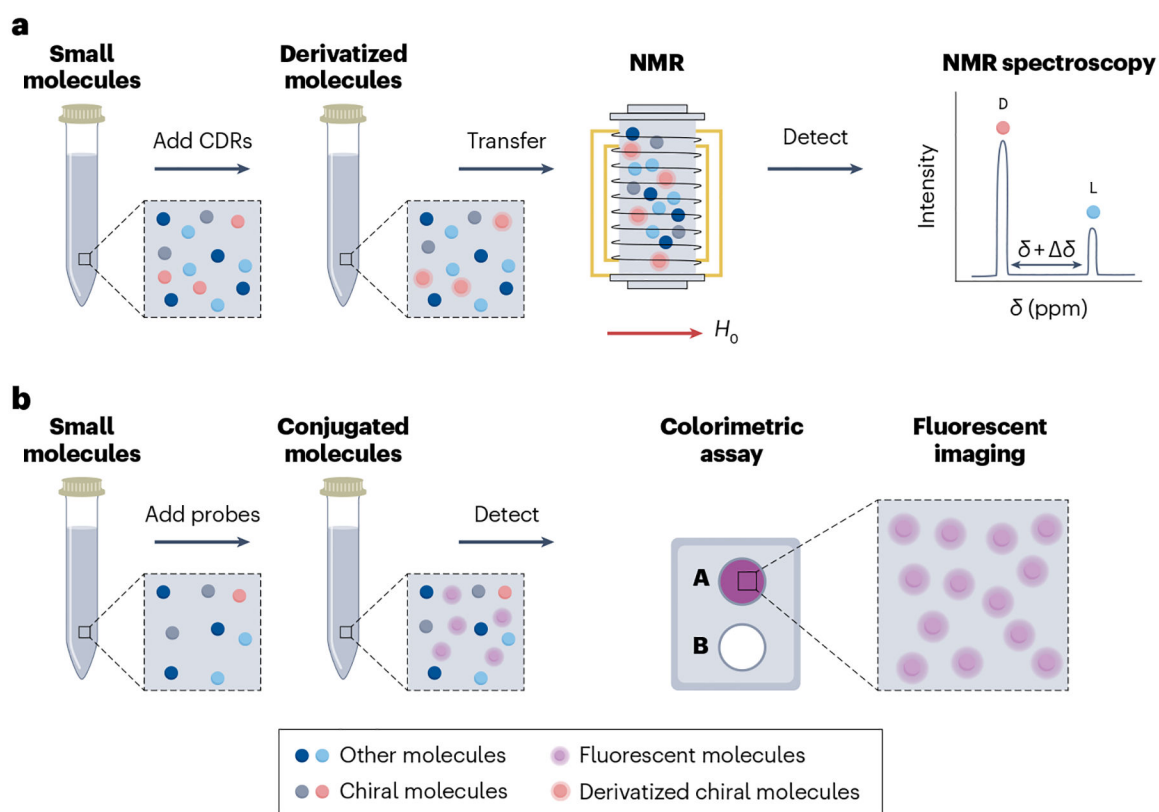


**Fig. 4 | Chiral detection of small molecules with NMR spectroscopy and an enzymatic assay.**  
**a**, After sample preparation, small molecules, with the addition of chiral derivatization reagents (CDRs), can be enantiomerically resolved using nuclear magnetic resonance (NMR) spectroscopy. The intensity between D and L peaks on the NMR spectrum reflects the enantiomeric excess. **b**, After sample preparation, enzymatic probes with enantiomeric selectivity are added to samples to form conjugated molecules. Fluorescent imaging of a colorimetric assay is used to determine the concentration of the targeted enantiomers.  $H_0$ , magnetic field.

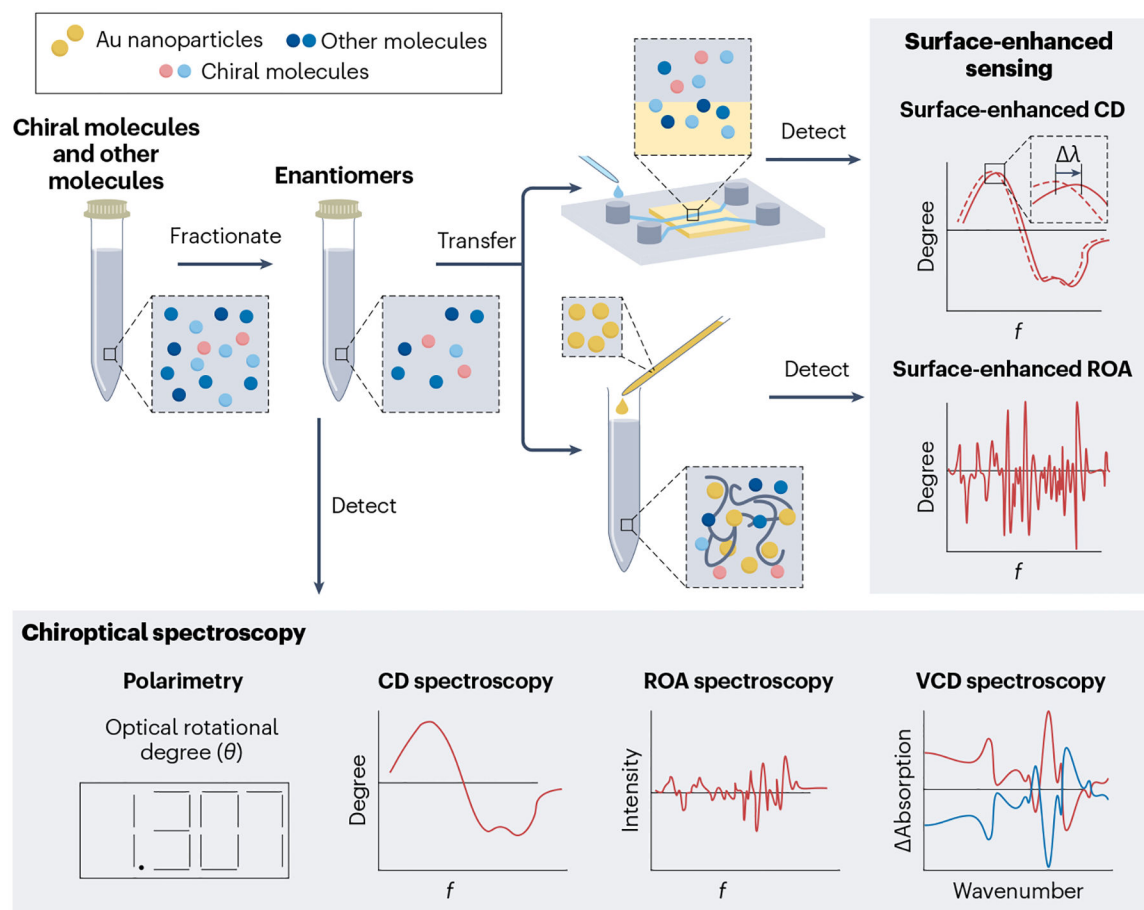


**Fig. 5 | Chiral detection using chiroptical spectroscopy.**

Several chiroptical methods and surface-enhanced strategies can be used to detect the chirality and stereochemical purity of small molecules.  $\lambda$ , wavelength; CD, circular dichroism;  $f$ , frequency; ROA, Raman optical activity; VCD, vibrational circular dichroism.



Table 1 |

Diseases and their associated abnormal chiral biomarkers

Disease	Biomarkers	Location	Concentrations in healthy subjects	Concentrations in patients
Cancer	Amino acids	D-Pro	6–30 $\mu\text{M}$ (ref. <sup>111</sup> ) <sup>a</sup>	2–110 $\mu\text{M}$ (ref. <sup>111</sup> ) <sup>a</sup>
		Saliva	0–11.3 $\mu\text{M}$ (ref. <sup>207</sup> ) <sup>b</sup>	22.5–112.6 $\mu\text{M}$ (ref. <sup>207</sup> ) <sup>b</sup>
	D-Ala	Gastric juice	5–24 $\mu\text{M}$ (ref. <sup>111</sup> ) <sup>a</sup>	20–280 $\mu\text{M}$ (ref. <sup>111</sup> ) <sup>a</sup>
		Saliva	0–25.3 $\mu\text{M}$ (ref. <sup>207</sup> ) <sup>b</sup>	50.6–253.2 $\mu\text{M}$ (ref. <sup>207</sup> ) <sup>b</sup>
	D-GLu	Gastric juice	0–0.8 $\mu\text{M}$ (ref. <sup>111</sup> ) <sup>a</sup>	0.4–1.7 $\mu\text{M}$ (ref. <sup>111</sup> ) <sup>a</sup>
		Serum	0.003–0.008 $\mu\text{M}$ (ref. <sup>112</sup> ) <sup>c</sup>	0.002–0.004 $\mu\text{M}$ (ref. <sup>112</sup> ) <sup>c</sup>
	D-Ser	Gastric juice	0.3–5.7 $\mu\text{M}$ (ref. <sup>111</sup> ) <sup>a</sup>	2–34 $\mu\text{M}$ (ref. <sup>111</sup> ) <sup>a</sup>
		Serum	0.013–0.03 $\mu\text{M}$ (ref. <sup>112</sup> ) <sup>c</sup>	0.005–0.019 $\mu\text{M}$ (ref. <sup>112</sup> ) <sup>c</sup>
	D-2-HG	Urine	2.8–17 $\text{mmolmol}^{-1}$ (ref. <sup>181</sup> ) <sup>d</sup>	4.1–2,668 $\text{mmolmol}^{-1}$ (ref. <sup>181</sup> ) <sup>d</sup>
			2.5–12 $\text{mmolmol}^{-1}$ (ref. <sup>104</sup> ) <sup>c</sup>	146–995 $\text{mmolmol}^{-1}$ (ref. <sup>267</sup> ) <sup>c</sup>
Serum	Serum	1–1.2 $\mu\text{M}$ (ref. <sup>268</sup> ) <sup>d</sup>	0.7–4.4 $\mu\text{M}$ (ref. <sup>268</sup> ) <sup>d</sup>	
		0.5–0.8 $\mu\text{M}$ (ref. <sup>269</sup> ) <sup>c</sup>	2.3–28 $\mu\text{M}$ (ref. <sup>269</sup> ) <sup>c</sup>	
		0.3–0.9 $\mu\text{M}$ (ref. <sup>181</sup> ) <sup>d</sup>	0.3–73 $\mu\text{M}$ (ref. <sup>181</sup> ) <sup>d</sup>	
Plasma	Plasma	0–26 $\mu\text{M}$ (ref. <sup>270</sup> ) <sup>d</sup>		
		0.1–0.4 $\mu\text{M}$ (ref. <sup>109</sup> ) <sup>c</sup>		
		2.4–14 $\text{mmolmol}^{-1}$ (ref. <sup>104</sup> ) <sup>c</sup>	2–22 $\text{mmolmol}^{-1}$ (ref. <sup>104</sup> ) <sup>c</sup>	
L-2-HG	Urine	1.3–19 $\text{mmolmol}^{-1}$ (ref. <sup>271</sup> ) <sup>d</sup>	4.1–2,742 $\text{mmolmol}^{-1}$ (ref. <sup>271</sup> ) <sup>d</sup>	
		0–5.2 $\text{mmolmol}^{-1}$ (ref. <sup>181</sup> ) <sup>d</sup>	41–158 $\text{mmolmol}^{-1}$ (ref. <sup>267</sup> ) <sup>c</sup>	
			121–471 $\text{mmolmol}^{-1}$ (ref. <sup>272</sup> ) <sup>c</sup>	
Serum	Serum	1–1.22 $\mu\text{M}$ (ref. <sup>268</sup> ) <sup>d</sup>	1.2–5.8 $\mu\text{M}$ (ref. <sup>268</sup> ) <sup>d</sup>	
		0.4–0.8 $\mu\text{M}$ (ref. <sup>269</sup> ) <sup>c</sup>	0.4–2.1 $\mu\text{M}$ (ref. <sup>269</sup> ) <sup>c</sup>	
		0–1.2 $\mu\text{M}$ (ref. <sup>269</sup> ) <sup>d</sup>		
Plasma	Plasma	0.5–1.0 $\mu\text{M}$ (ref. <sup>181</sup> ) <sup>d</sup>	0.3–1.7 $\mu\text{M}$ (ref. <sup>181</sup> ) <sup>d</sup>	
Brain diseases	Amino acids	D-Asp	15–22.2 $\text{nmolg}^{-1}$ (ref. <sup>84</sup> ) <sup>b</sup>	8.9–20.7 $\text{nmolg}^{-1}$ (ref. <sup>84</sup> ) <sup>b</sup>
		Grey matter		

Disease	Biomarkers	Location	Concentrations in healthy subjects	Concentrations in patients
		White matter	17.8–27 nmol·g <sup>-1</sup> (ref. <sup>84</sup> ) <sup>b</sup>	3.9–17.1 nmol·g <sup>-1</sup> (ref. <sup>84</sup> ) <sup>b</sup>
			0.5–2.0 μM (ref. <sup>180</sup> ) <sup>b</sup>	1.2–5.4 μM (ref. <sup>180</sup> ) <sup>b</sup>
			0.5–1.6 μM (ref. <sup>273</sup> ) <sup>e</sup>	
D-Ala		Grey matter	16–26 nmol·g <sup>-1</sup> (ref. <sup>84</sup> ) <sup>b</sup>	7–12 nmol·g <sup>-1</sup> (ref. <sup>84</sup> ) <sup>b</sup>
		White matter	2–23 nmol·g <sup>-1</sup> (ref. <sup>84</sup> ) <sup>b</sup>	6–21 nmol·g <sup>-1</sup> (ref. <sup>84</sup> ) <sup>b</sup>
D-Ser		Serum	1.7–2.9 μM (ref. <sup>56</sup> ) <sup>c</sup>	1.3–2.4 μM (ref. <sup>56</sup> ) <sup>c</sup>
			0.9–2.2 μM (ref. <sup>72</sup> ) <sup>a</sup>	0.8–3.2 μM (ref. <sup>72</sup> ) <sup>a</sup>
			1.0–2.9 μM (ref. <sup>134</sup> ) <sup>d</sup>	1.4–2.4 μM (ref. <sup>274</sup> ) <sup>c</sup>
			1.5–2.8 μM (ref. <sup>274</sup> ) <sup>c</sup>	
		Plasma	1.4–2.5 μM (ref. <sup>275</sup> ) <sup>a</sup>	1.2–4.2 μM (ref. <sup>275</sup> ) <sup>a</sup>
			1.7–2.9 μM (ref. <sup>276</sup> ) <sup>a</sup>	
			0.6–1.3 μM (ref. <sup>277</sup> ) <sup>c</sup>	
		CSF	0.6–3.0 μM (ref. <sup>180</sup> ) <sup>b</sup>	4.9–13.1 μM (ref. <sup>180</sup> ) <sup>b</sup>
			1.8–11.7 μM (ref. <sup>278</sup> ) <sup>d</sup>	1.3–1.9 μM (ref. <sup>71</sup> ) <sup>c</sup>
			1.1–1.6 μM (ref. <sup>71</sup> ) <sup>c</sup>	0.9–1.8 μM (ref. <sup>33</sup> ) <sup>b</sup>
			1.4–2.2 μM (ref. <sup>33</sup> ) <sup>b</sup>	
Total <sup>f</sup>		CSF	12.5–23.3 μM (ref. <sup>180</sup> ) <sup>b</sup>	18.8–34 μM (ref. <sup>180</sup> ) <sup>b</sup>
Organic acids		D-2-HG	0.07–0.3 μM (ref. <sup>17</sup> ) <sup>d</sup>	0.42–6 μM (ref. <sup>17</sup> ) <sup>d</sup>
		Plasma	0.3–0.9 μM (ref. <sup>181</sup> ) <sup>d</sup>	2.2–26 μM (ref. <sup>17</sup> ) <sup>d</sup>
			0–26 μM (ref. <sup>270</sup> ) <sup>d</sup>	2.5–17 μM (ref. <sup>91</sup> ) <sup>d</sup>
			0.1–0.4 μM (ref. <sup>109</sup> ) <sup>c</sup>	
		Urine	2.8–17 mmolmol <sup>-1</sup> (ref. <sup>181</sup> ) <sup>d</sup>	228–750 mmolmol <sup>-1</sup> (ref. <sup>17</sup> ) <sup>d</sup>
			2.5–12 mmolmol <sup>-1</sup> (ref. <sup>104</sup> ) <sup>c</sup>	18–1,185 mmolmol <sup>-1</sup> (ref. <sup>91</sup> ) <sup>d</sup>
L-2-HG		Plasma	0.5–1.0 μM (ref. <sup>181</sup> ) <sup>d</sup>	1.1–3.0 μM (ref. <sup>17</sup> ) <sup>d</sup>
				2.2–3.7 μM (ref. <sup>91</sup> ) <sup>d</sup>
		Urine	2.4–14 mmolmol <sup>-1</sup> (ref. <sup>104</sup> ) <sup>c</sup>	630–1,420 mmolmol <sup>-1</sup> (ref. <sup>279</sup> ) <sup>d</sup>
			1.3–19 mmolmol <sup>-1</sup> (ref. <sup>271</sup> ) <sup>d</sup>	1,000–5,520 mmolmol <sup>-1</sup> (ref. <sup>280</sup> ) <sup>c</sup>
			0–52 mmolmol <sup>-1</sup> (ref. <sup>181</sup> ) <sup>d</sup>	

Disease	Biomarkers	Location	Concentrations in healthy subjects	Concentrations in patients
Kidney diseases and diabetes	Amino acids	D-Asn	Plasma	25.2–430 mmol mol <sup>-1</sup> (ref. <sup>91</sup> ) <sup>d</sup>
				671–3,392 mmol mol <sup>-1</sup> (ref. <sup>281</sup> ) <sup>d</sup>
	D-Ser	Plasma	0–0.12 μM (ref. <sup>277</sup> ) <sup>c</sup>	0.14–0.36 μM (ref. <sup>186</sup> ) <sup>c</sup>
			0.02–0.18 μM (ref. <sup>277</sup> ) <sup>c</sup>	
			1.4–2.5 μM (ref. <sup>275</sup> ) <sup>a</sup>	1.76–3.13 μM (ref. <sup>186</sup> ) <sup>c</sup>
			1.7–2.9 μM (ref. <sup>276</sup> ) <sup>a</sup>	
	D-Ala	Plasma	0.6–1.3 μM (ref. <sup>277</sup> ) <sup>c</sup>	
			0–0.14 μM (ref. <sup>277</sup> ) <sup>c</sup>	1.18–4.73 μM (ref. <sup>186</sup> ) <sup>c</sup>
			1.21–2.43 μM (ref. <sup>282</sup> ) <sup>e</sup>	
	D-Pro	Plasma	0–14.6 pmolmg <sup>-1</sup> (ref. <sup>101</sup> ) <sup>c</sup>	3.6–49.5 pmolmg <sup>-1</sup> (ref. <sup>101</sup> ) <sup>c</sup>
			0–0.7 μM (ref. <sup>186</sup> ) <sup>c</sup>	0.80–0.88 μM (ref. <sup>186</sup> ) <sup>c</sup>
	D-Tyr	Plasma	0.15–0.56 μM (ref. <sup>277</sup> ) <sup>c</sup>	
			0.3–2.3 pmolmg <sup>-1</sup> (ref. <sup>101</sup> ) <sup>c</sup>	0–7.8 pmolmg <sup>-1</sup> (ref. <sup>101</sup> ) <sup>c</sup>
	D-Phe	Plasma	0.7–1.1 μM (ref. <sup>100</sup> ) <sup>b</sup>	0.8–5.6 μM (ref. <sup>100</sup> ) <sup>b</sup>
			0–0.12 μM (ref. <sup>277</sup> ) <sup>c</sup>	
	D-Val	Nail	0.3–0.7 μM (ref. <sup>100</sup> ) <sup>b</sup>	0.1–3.5 μM (ref. <sup>100</sup> ) <sup>b</sup>
			0.10–0.30 μM (ref. <sup>277</sup> ) <sup>c</sup>	
	D-Ile	Nail	0.1–0.4 pmolmg <sup>-1</sup> (ref. <sup>101</sup> ) <sup>c</sup>	0–14.8 pmolmg <sup>-1</sup> (ref. <sup>101</sup> ) <sup>c</sup>
			0.1–0.4 pmolmg <sup>-1</sup> (ref. <sup>101</sup> ) <sup>c</sup>	0–6.4 pmolmg <sup>-1</sup> (ref. <sup>101</sup> ) <sup>c</sup>
	D-Leu	Nail	1.3–3.8 pmolmg <sup>-1</sup> (ref. <sup>101</sup> ) <sup>c</sup>	0–35.6 pmolmg <sup>-1</sup> (ref. <sup>101</sup> ) <sup>c</sup>
Organic acids	D-Lac	Plasma	7.4–8.6 μM (ref. <sup>283</sup> ) <sup>c</sup>	9.5–11.9 μM (ref. <sup>283</sup> ) <sup>c</sup>
			21.0–25.0 μM (ref. <sup>284</sup> ) <sup>b</sup>	15.9–63.3 μM (ref. <sup>18</sup> ) <sup>b</sup>
	Urine		0.9–1.3 mmolmol <sup>-1</sup> (ref. <sup>283</sup> ) <sup>c</sup>	2.3–3.9 mmolmol <sup>-1</sup> (ref. <sup>283</sup> ) <sup>c</sup>
			6.2–30.2 mmolmol <sup>-1</sup> (ref. <sup>18</sup> ) <sup>b</sup>	11.7–60.1 mmolmol <sup>-1</sup> (ref. <sup>18</sup> ) <sup>b</sup>
	D-HA	Saliva	0.02–0.11 μM (ref. <sup>285</sup> ) <sup>c</sup>	0.00–0.96 μM (ref. <sup>285</sup> ) <sup>c</sup>
			0.02–0.10 μM (ref. <sup>285</sup> ) <sup>c</sup>	0.13–0.34 μM (ref. <sup>285</sup> ) <sup>c</sup>

Disease	Biomarkers	Location	Concentrations in healthy subjects	Concentrations in patients
	D-2-HG	Urine	2.8–17 mmolmol <sup>-1</sup> (ref. <sup>181</sup> ) <sup>d</sup> 2.5–12 mmolmol <sup>-1</sup> (ref. <sup>104</sup> ) <sup>c</sup>	0.2–16.5 mmolmol <sup>-1</sup> (ref. <sup>104</sup> ) <sup>c</sup>
	L-2-HG	Urine	2.4–14 mmolmol <sup>-1</sup> (ref. <sup>104</sup> ) <sup>c</sup> 1.3–19 mmolmol <sup>-1</sup> (ref. <sup>271</sup> ) <sup>d</sup> 0–52 mmolmol <sup>-1</sup> (ref. <sup>181</sup> ) <sup>d</sup>	0.1–22.5 mmolmol <sup>-1</sup> (ref. <sup>104</sup> ) <sup>c</sup>

2-HG, 2-hydroxyglutarate; CSF, cerebrospinal fluid; D-HA, D-3-hydroxybutyric acid; D-Lac, D-lactate.

<sup>a</sup>Concentrations determined by liquid chromatography–fluorescence.

<sup>b</sup>Concentrations determined by enzymatic assay.

<sup>c</sup>Concentrations determined by liquid chromatography–mass spectrometry.

<sup>d</sup>Concentrations determined by gas chromatography–mass spectrometry.

<sup>e</sup>Concentrations determined by capillary electrophoresis–fluorescence.

<sup>f</sup>Total concentration of D-amino acids.

Table 2 |

## Comparison of chiral detection techniques

Method	Limit of detection	Sample quantity	Clinical sample type	Number of measurable metabolites per run	Cost	Diseases	Level of development
Chromatography <sup>152,177-179,185,189,286,287</sup>	100 pM (refs. <sup>185,287</sup> )	10 µL-100 ml	Serum, plasma, urine, CSF, saliva, tissue	1-20	Medium	Cancer, brain diseases, kidney disease, diabetes	Well developed
Capillary electrophoresis <sup>139,192-195,288</sup>	5nM (refs. <sup>193-288</sup> )	100 nL-1 ml	Serum, plasma, urine, glial vesicles, tissue	1-20	Low	Brain diseases	Well developed
NMR spectroscopy <sup>200-202,204</sup>	10 nM (refs. <sup>202,204</sup> )	10 µL-100 ml	Urine	1-20	High	Brain diseases	Under development
Enzymatic assay <sup>21,205-208</sup>	200 nM (ref. <sup>289</sup> )	10 µL-10 ml	Serum, CSF, plasma, urine, saliva, tissue	1	Low	Cancer, brain diseases, kidney disease, diabetes	Well developed
Polarimetry <sup>142-144,214</sup>	1 mM (refs. <sup>143,214</sup> )	10 ml	Blood	1	Low	Diabetes	Under development
CD spectroscopy <sup>145,217</sup>	5 µM (refs. <sup>145,217</sup> )	100 µL-100 ml	CSF, tissue	1	Low	Brain diseases	Under development
ROA spectroscopy <sup>222-226</sup>	0.2 mM (ref. <sup>226</sup> )	100 µL-100 ml	-	1	Medium	-	Under development
VCD spectroscopy <sup>227-230</sup>	5 mM (ref. <sup>230</sup> )	100 µL-100 ml	-	1	Medium	-	Under development
Surface-enhanced CD spectroscopy <sup>233-236,240,244</sup>	20 pM (refs. <sup>240,244</sup> )	10 µL-100 µL	Tissue, urine	1	Low	Brain diseases, diabetes	Under development
Surface-enhanced ROA spectroscopy <sup>245,246</sup>	100 nM (ref. <sup>246</sup> )	10 µL-1 ml	-	1	Low	-	Under development

CD, circular dichroism; CSF, cerebrospinal fluid; NMR, nuclear magnetic resonance; ROA, Raman optical activity; VCD, vibrational circular dichroism.